Alken *et al. Earth, Planets and Space* (2021) 73:49
https://doi.org/10.1186/s40623-020-01288-x

Earth, Planets and Space

FULL PAPER

International Geomagnetic Reference Field: the thirteenth generation

P. Alken[1,2*], E. Thébault[3], C. D. Beggan[4], H. Amit[3], J. Aubert[6], J. Baerenzung[22], T. N. Bondar[17], W. J. Brown[4], S. Califf[1,2], A. Chambodut[12], A. Chulliat[1,2], G. A. Cox[4], C. C. Finlay[5], A. Fournier[6], N. Gillet[7], A. Grayver[28], M. D. Hammer[5], M. Holschneider[22], L. Huder[7], G. Hulot[6], T. Jager[16], C. Kloss[5], M. Korte[10], W. Kuang[23], A. Kuvshinov[28], B. Langlais[3], J.-M. Léger[16], V. Lesur[6], P. W. Livermore[8], F. J. Lowes[9], S. Macmillan[4], W. Magnes[15], M. Mandea[27], S. Marsal[26], J. Matzka[10], M. C. Metman[8], T. Minami[18,20], A. Morschhauser[10], J. E. Mound[8], M. Nair[1,2], S. Nakano[19], N. Olsen[5], F. J. Pavón-Carrasco[24,25], V. G. Petrov[17], G. Ropp[6], M. Rother[10], T. J. Sabaka[23], S. Sanchez[21], D. Saturnino[3], N. R. Schnepf[1,2], X. Shen[13], C. Stolle[10], A. Tangborn[23], L. Tøffner-Clausen[5], H. Toh[11], J. M. Torta[26], J. Varner[1,2], F. Vervelidou[10], P. Vigneron[6], I. Wardinski[12], J. Wicht[21], A. Woods[1,2], Y. Yang[13], Z. Zeren[13] and B. Zhou[14]

Abstract
In December 2019, the International Association of Geomagnetism and Aeronomy (IAGA) Division V Working Group (V-MOD) adopted the thirteenth generation of the International Geomagnetic Reference Field (IGRF). This IGRF updates the previous generation with a definitive main field model for epoch 2015.0, a main field model for epoch 2020.0, and a predictive linear secular variation for 2020.0 to 2025.0. This letter provides the equations defining the IGRF, the spherical harmonic coefficients for this thirteenth generation model, maps of magnetic declination, inclination and total field intensity for the epoch 2020.0, and maps of their predicted rate of change for the 2020.0 to 2025.0 time period.

Keywords: IGRF, Magnetic field modeling, Geomagnetism

Introduction

The International Geomagnetic Reference Field (IGRF) is a set of spherical harmonic coefficients which can be input into a mathematical model in order to describe the large-scale, time-varying portion of Earth's internal magnetic field between epochs 1900 A.D. and the present. The IGRF is produced and maintained by an international task force of scientists under the auspices of the International Association of Geomagnetism and Aeronomy (IAGA) Working Group V-MOD. This thirteenth generation IGRF has been derived from observations recorded by satellites, ground observatories, and magnetic surveys (see Appendix 1 for a list of World Data System data centers and services). IGRF is routinely used by the scientific community to study Earth's core field, space weather, electromagnetic induction, and local magnetic anomalies in the lithosphere. It is also widely used in satellite attitude determination and control systems and other applications requiring orientation information.

Earth's core field changes continuously and unpredictably on timescales ranging from months to millions of years. In order to account for temporal changes on timescales of a few years, the IGRF is regularly revised, typically every 5 years. Table 1 summarizes the current and past generations of IGRF. Each generation is composed of a set of model coefficients representing the internal time-varying geomagnetic field, which are provided in 5-year intervals. The years for which coefficients are provided are called *model epochs*. The coefficients of a certain epoch represent a snapshot of the geomagnetic field at that time, and can be labeled either as a Definitive Geomagnetic Reference Model (DGRF) or as an IGRF.

*Correspondence: alken@colorado.edu
[2] NOAA National Centers for Environmental Information, Boulder, CO, USA
Full list of author information is available at the end of the article

Table 1 Summary of IGRF generations, validity periods, release years, and references

Full name	Short name	Validity period	Definitive period	Release year	Reference
IGRF 13th generation	IGRF-13	1900.0 to 2025.0	1945.0 to 2015.0	2019	This article
IGRF 12th generation	IGRF-12	1900.0 to 2020.0	1945.0 to 2010.0	2014	Thébault et al. (2015)
IGRF 11th generation	IGRF-11	1900.0 to 2015.0	1945.0 to 2005.0	2009	Finlay et al. (2010a)
IGRF 10th generation	IGRF-10	1900.0 to 2010.0	1945.0 to 2000.0	2004	Maus et al. (2005); Macmillan and Maus (2005)
IGRF 9th generation	IGRF-9	1900.0 to 2005.0	1945.0 to 2000.0	2003	Macmillan et al. (2003)
IGRF 8th generation	IGRF-8	1900.0 to 2005.0	1945.0 to 1990.0	1999	Mandea and Macmillan (2000)
IGRF 7th generation	IGRF-7	1900.0 to 2000.0	1945.0 to 1990.0	1995	Barton (1997)
IGRF 6th generation	IGRF-6	1945.0 to 1995.0	1945.0 to 1985.0	1991	Langel (1992)
IGRF 5th generation	IGRF-5	1945.0 to 1990.0	1945.0 to 1980.0	1987	Barraclough et al. (1987); Langel et al. (1988)
IGRF 4th generation	IGRF-4	1945.0 to 1990.0	1965.0 to 1980.0	1985	Barraclough (1987)
IGRF 3rd generation	IGRF-3	1965.0 to 1985.0	1965.0 to 1975.0	1981	Peddie (1982)
IGRF 2nd generation	IGRF-2	1955.0 to 1980.0	-	1975	IAGA Division I Study Group (1975)
IGRF 1st generation	IGRF-1	1955.0 to 1975.0	-	1968	Cain and Cain (1971); Zmuda (1971a, 1971b)

DGRF models are so labeled because they have been built from the best available data sources of that time period and therefore are unlikely to be improved in future IGRF revisions. Models labeled as IGRF are non-definitive, and will likely be revised in the future as more data are collected. DGRF models have been built only starting in 1945. Details of the history of IGRF can be found in Barton (1997) and Macmillan and Finlay (2011). Past generations of IGRF models are archived at https://www.ngdc.noaa.gov/IAGA/vmod/igrf_old_models.html. Since later IGRFs can revise model parameters for past epochs, it is important to record which generation of IGRF was used to process a particular dataset, so that the original data can be recovered and reprocessed with the latest generation of IGRF if needed.

In this paper, we focus on the thirteenth generation of IGRF, known hereafter as IGRF-13. IGRF-13 provides a DGRF model for epoch 2015.0, an IGRF model for epoch 2020.0, and a predictive IGRF secular variation model for the 5-year time interval 2020.0 to 2025.0. For epochs 1900.0 to 2010.0, the IGRF-13 model coefficients are unchanged from IGRF-12. IGRF-13 was finalized in December 2019 by a task force of IAGA Working Group V-MOD. In the following sections, we will describe the IGRF model, provide the final set of IGRF-13 coefficients, and briefly discuss large-scale features of the geomagnetic field at Earth's surface as revealed by the updated model.

Mathematical formulation of the IGRF model

The IGRF describes the main geomagnetic field $\mathbf{B}(r,\theta,\phi,t)$ which is produced by internal sources primarily inside Earth's core. The IGRF is valid on and above Earth's surface, where the main geomagnetic field can be described as the gradient of a scalar potential, $\mathbf{B} = -\nabla V$, and the potential function $V(r,\theta,\phi,t)$ is represented as a finite series expansion in terms of spherical harmonic coefficients, g_n^m, h_n^m, also known as the *Gauss coefficients*:

$$V(r,\theta,\phi,t) = a \sum_{n=1}^{N} \sum_{m=0}^{n} \left(\frac{a}{r}\right)^{n+1} \cdot \left[{g_n}^m(t) \cos m\phi + {h_n}^m(t) \sin m\phi \right] {P_n}^m(\cos\theta) \quad (1)$$

Here, r,θ,ϕ refer to coordinates in a geocentric spherical coordinate system, with r being radial distance from the center of the Earth, and θ,ϕ representing geocentric co-latitude and longitude, respectively. A reference radius $a = 6371.2$ km is chosen to approximate the mean Earth radius. The $P_n^m(\cos\theta)$ are Schmidt semi-normalized associated Legendre functions of degree n and order m (Winch et al. 2005). The parameter N specifies the maximum spherical harmonic degree of expansion, and was chosen to be 10 up to and including epoch 1995, after which it increases to 13 to account for the smaller scale internal signals which can be captured by high-resolution satellite missions such as Ørsted, CHAMP and Swarm. The Gauss coefficients $g_n^m(t), h_n^m(t)$ change in time and are provided in units of nanoTesla (nT) in IGRF-13 at 5-year epoch intervals. The time dependence of these parameters is modeled as piecewise linear, and is given by

$$g_n^m(t) = g_n^m(T_t) + (t - T_t)\dot{g}_n^m(T_t), \quad (2)$$

$$h_n^m(t) = h_n^m(T_t) + (t - T_t)\dot{h}_n^m(T_t), \quad (3)$$

where $g_n^m(T_t), h_n^m(T_t)$ are the Gauss coefficients at epoch T_t, which immediately precedes time t. The model epochs in IGRF-13 are provided in exact multiples of 5 years starting in 1900 and ending in 2020 (see Table 2), so that $T_t \leq t < T_t + 5$. For $T_t < 2020$, the parameters

Table 2 13th generation International Geomagnetic Reference Field

g/h	Deg n	Ord m	IGRF 1900.0	IGRF 1905.0	IGRF 1910.0	IGRF 1915.0	IGRF 1920.0	IGRF 1925.0	IGRF 1930.0	IGRF 1935.0	IGRF 1940.0	DGRF 1945.0	DGRF 1950.0	DGRF 1955.0	DGRF 1960.0
g	1	0	−31543	−31464	−31354	−31212	−31060	−30926	−30805	−30715	−30654	−30594	−30554	−30500	−30421
g	1	1	−2298	−2298	−2297	−2306	−2317	−2318	−2316	−2306	−2292	−2285	−2250	−2215	−2169
h	1	1	5922	5909	5898	5875	5845	5817	5808	5812	5821	5810	5815	5820	5791
g	2	0	−677	−728	−769	−802	−839	−893	−951	−1018	−1106	−1244	−1341	−1440	−1555
g	2	1	2905	2928	2948	2956	2959	2969	2980	2984	2981	2990	2998	3003	3002
h	2	1	−1061	−1086	−1128	−1191	−1259	−1334	−1424	−1520	−1614	−1702	−1810	−1898	−1967
g	2	2	924	1041	1176	1309	1407	1471	1517	1550	1566	1578	1576	1581	1590
h	2	2	1121	1065	1000	917	823	728	644	586	528	477	381	291	206
g	3	0	1022	1037	1058	1084	1111	1140	1172	1206	1240	1282	1297	1302	1302
g	3	1	−1469	−1494	−1524	−1559	−1600	−1645	−1692	−1740	−1790	−1834	−1889	−1944	−1992
h	3	1	−330	−357	−389	−421	−445	−462	−480	−494	−499	−499	−476	−462	−414
g	3	2	1256	1239	1223	1212	1205	1202	1205	1215	1232	1255	1274	1288	1289
h	3	2	3	34	62	84	103	119	133	146	163	186	206	216	224
g	3	3	572	635	705	778	839	881	907	918	916	913	896	882	878
h	3	3	523	480	425	360	293	229	166	101	43	−11	−46	−83	−130
g	4	0	876	880	884	887	889	891	896	903	914	944	954	958	957
g	4	1	628	643	660	678	695	711	727	744	762	776	792	796	800
h	4	1	195	203	211	218	220	216	205	188	169	144	136	133	135
g	4	2	660	653	644	631	616	601	584	565	550	544	528	510	504
h	4	2	−69	−77	−90	−109	−134	−163	−195	−226	−252	−276	−278	−274	−278
g	4	3	−361	−380	−400	−416	−424	−426	−422	−415	−405	−421	−408	−397	−394
h	4	3	−210	−201	−189	−173	−153	−130	−109	−90	−72	−55	−37	−23	3
g	4	4	134	146	160	178	199	217	234	249	265	304	303	290	269
h	4	4	−75	−65	−55	−51	−57	−70	−90	−114	−141	−178	−210	−230	−255
g	5	0	−184	−192	−201	−211	−221	−230	−237	−241	−241	−253	−240	−229	−222
g	5	1	328	328	327	327	326	326	327	329	334	346	349	360	362
h	5	1	−210	−193	−172	−148	−122	−96	−72	−51	−33	−12	3	15	16
g	5	2	264	259	253	245	236	226	218	211	208	194	211	230	242
h	5	2	53	56	57	58	58	58	60	64	71	95	103	110	125
g	5	3	5	−1	−9	−16	−23	−28	−32	−33	−33	−20	−20	−23	−26
h	5	3	−33	−32	−33	−34	−38	−44	−53	−64	−75	−67	−87	−98	−117
g	5	4	−86	−93	−102	−111	−119	−125	−131	−136	−141	−142	−147	−152	−156
h	5	4	−124	−125	−126	−126	−125	−122	−118	−115	−113	−119	−122	−121	−114
g	5	5	−16	−26	−38	−51	−62	−69	−74	−76	−76	−82	−76	−69	−63
h	5	5	3	11	21	32	43	51	58	64	69	82	80	78	81
g	6	0	63	62	62	61	61	61	60	59	57	59	54	47	46
g	6	1	61	60	58	57	55	54	53	53	54	57	57	57	58

Table 2 (continued)

g/h	Deg n	Ord m	IGRF 1900.0	IGRF 1905.0	IGRF 1910.0	IGRF 1915.0	IGRF 1920.0	IGRF 1925.0	IGRF 1930.0	IGRF 1935.0	IGRF 1940.0	DGRF 1945.0	DGRF 1950.0	DGRF 1955.0	DGRF 1960.0
h	6	1	−9	−7	−5	−2	0	3	4	4	4	6	−1	−9	−10
g	6	2	−11	−11	−11	−10	−10	−9	−9	−8	−7	6	4	3	1
h	6	2	83	86	89	93	96	99	102	104	105	100	99	96	99
g	6	3	−217	−221	−224	−228	−233	−238	−242	−246	−249	−246	−247	−247	−237
h	6	3	2	4	5	8	11	14	19	25	33	16	33	48	60
g	6	4	−58	−57	−54	−51	−46	−40	−32	−25	−18	−25	−16	−8	−1
h	6	4	−35	−32	−29	−26	−22	−18	−16	−15	−15	−9	−12	−16	−20
g	6	5	59	57	54	49	44	39	32	25	18	21	12	7	−2
h	6	5	36	32	28	23	18	13	8	4	0	−16	−12	−12	−11
g	6	6	−90	−92	−95	−98	−101	−103	−104	−106	−107	−104	−105	−107	−113
h	6	6	−69	−67	−65	−62	−57	−52	−46	−40	−33	−39	−30	−24	−17
g	7	0	70	70	71	72	73	73	74	74	74	70	65	65	67
g	7	1	−55	−54	−54	−54	−54	−54	−54	−53	−53	−40	−55	−56	−56
h	7	1	−45	−46	−47	−48	−49	−50	−51	−52	−52	−45	−35	−50	−55
g	7	2	0	0	1	2	2	3	4	4	4	0	2	2	5
h	7	2	−13	−14	−14	−14	−14	−14	−15	−17	−18	−18	−17	−24	−28
g	7	3	34	33	32	31	29	27	25	23	20	0	1	10	15
h	7	3	−10	−11	−12	−12	−13	−14	−14	−14	−14	2	0	−4	−6
g	7	4	−41	−41	−40	−38	−37	−35	−34	−33	−31	−29	−40	−32	−32
h	7	4	−1	0	1	2	4	5	6	7	7	6	10	8	7
g	7	5	−21	−20	−19	−18	−16	−14	−12	−11	−9	−10	−7	−11	−7
h	7	5	28	28	28	28	28	29	29	29	29	28	36	28	23
g	7	6	18	18	18	19	19	19	18	18	17	15	5	9	17
h	7	6	−12	−12	−13	−15	−16	−17	−18	−19	−20	−17	−18	−20	−18
g	7	7	6	6	6	6	6	6	6	6	5	29	19	18	8
h	7	7	−22	−22	−22	−22	−22	−21	−20	−19	−19	−22	−16	−18	−17
g	8	0	11	11	11	11	11	11	11	11	11	13	22	11	15
g	8	1	8	8	8	8	7	7	7	7	7	7	15	9	6
h	8	1	8	8	8	8	8	8	8	8	8	12	5	10	11
g	8	2	−4	−4	−4	−4	−3	−3	−3	−3	−3	−8	−4	−6	−4
h	8	2	−14	−15	−15	−15	−15	−15	−15	−15	−14	−21	−22	−15	−14
g	8	3	−9	−9	−9	−9	−9	−9	−9	−9	−10	−5	−1	−14	−11
h	8	3	7	7	6	6	6	6	5	5	5	−12	0	5	7
g	8	4	1	1	1	2	2	2	2	1	1	9	11	6	2
h	8	4	−13	−13	−13	−13	−14	−14	−14	−15	−15	−7	−21	−23	−18
g	8	5	2	2	2	3	4	4	5	6	6	7	15	10	10

Table 2 (continued)

g/h	Deg n	Ord m	IGRF 1900.0	IGRF 1905.0	IGRF 1910.0	IGRF 1915.0	IGRF 1920.0	IGRF 1925.0	IGRF 1930.0	IGRF 1935.0	IGRF 1940.0	DGRF 1945.0	DGRF 1950.0	DGRF 1955.0	DGRF 1960.0
h	8	5	5	5	5	5	5	5	5	5	5	2	−8	3	4
g	8	6	−9	−8	−8	−8	−7	−7	−6	−6	−5	−10	−13	−7	−5
h	8	6	16	16	16	16	17	17	18	18	19	18	17	23	23
g	8	7	5	5	5	6	6	7	8	8	9	7	5	6	10
h	8	7	−5	−5	−5	−5	−5	−5	−5	−5	−5	3	−4	−4	1
g	8	8	8	8	8	8	8	8	8	7	7	2	−1	9	8
h	8	8	−18	−18	−18	−18	−19	−19	−19	−19	−19	−11	−17	−13	−20
g	9	0	8	8	8	8	8	8	8	8	8	5	3	4	4
g	9	1	10	10	10	10	10	10	10	10	10	−21	−7	9	6
h	9	1	−20	−20	−20	−20	−20	−20	−20	−20	−21	−27	−24	−11	−18
g	9	2	1	1	1	1	1	1	1	1	1	1	−1	−4	0
h	9	2	14	14	14	14	14	14	14	15	15	17	19	12	12
g	9	3	−11	−11	−11	−11	−11	−11	−12	−12	−12	−11	−25	−5	−9
h	9	3	5	5	5	5	5	5	5	5	5	29	12	7	2
g	9	4	12	12	12	12	12	12	12	11	11	3	10	2	1
h	9	4	−3	−3	−3	−3	−3	−3	−3	−3	−3	−9	2	6	0
g	9	5	1	1	1	1	1	1	1	1	1	16	5	4	4
h	9	5	−2	−2	−2	−2	−2	−2	−2	−3	−3	4	2	−2	−3
g	9	6	−2	−2	−2	−2	−2	−2	−2	−2	−2	−3	−5	1	−1
h	9	6	8	8	8	8	9	9	9	9	9	9	8	10	9
g	9	7	2	2	2	2	2	2	3	3	3	−4	−2	2	−2
h	9	7	10	10	10	10	10	10	10	11	11	6	8	7	8
g	9	8	−1	0	0	0	0	0	0	0	1	−3	3	2	3
h	9	8	−2	−2	−2	−2	−2	−2	−2	−2	−2	1	−11	−6	0
g	9	9	−1	−1	−1	−1	−1	−1	−2	−2	−2	−4	8	5	−1
h	9	9	2	2	2	2	2	2	2	2	2	8	−7	5	5
g	10	0	−3	−3	−3	−3	−3	−3	−3	−3	−3	−3	−8	−3	1
g	10	1	−4	−4	−4	−4	−4	−4	−4	−4	−4	11	4	−5	−3
h	10	1	2	2	2	2	2	2	2	2	2	5	13	−4	4
g	10	2	2	2	2	2	2	2	2	2	2	1	−1	−1	4
h	10	2	1	1	1	1	1	1	1	1	1	1	−2	0	1
g	10	3	−5	−5	−5	−5	−5	−5	−5	−5	−5	2	13	2	0
h	10	3	2	2	2	2	2	2	2	2	2	−20	−10	−8	0
g	10	4	−2	−2	−2	−2	−2	−2	−2	−2	−2	−5	−4	−3	−1
h	10	4	6	6	6	6	6	6	6	6	6	−1	2	−2	2

Table 2 (continued)

g/h	Deg n	Ord m	IGRF 1900.0	IGRF 1905.0	IGRF 1910.0	IGRF 1915.0	IGRF 1920.0	IGRF 1925.0	IGRF 1930.0	IGRF 1935.0	IGRF 1940.0	DGRF 1945.0	DGRF 1950.0	DGRF 1955.0	DGRF 1960.0
g	10	5	6	6	6	6	6	6	6	6	6	−1	4	7	4
h	10	5	−4	−4	−4	−4	−4	−4	−4	−4	−4	−6	−3	−4	−5
g	10	6	4	4	4	4	4	4	4	4	4	8	12	4	6
h	10	6	0	0	0	0	0	0	0	0	0	6	6	1	1
g	10	7	0	0	0	0	0	0	0	0	0	−1	3	−2	1
h	10	7	−2	−2	−2	−2	−2	−2	−2	−1	−1	−4	−3	−3	−1
g	10	8	2	2	2	1	1	1	1	2	2	−3	2	6	−1
h	10	8	4	4	4	4	4	4	4	4	4	−2	6	7	6
g	10	9	2	2	2	2	3	3	3	3	3	5	10	−2	2
h	10	9	0	0	0	0	0	0	0	0	0	0	11	−1	0
g	10	10	0	0	0	0	0	0	0	0	0	−2	3	0	0
h	10	10	−6	−6	−6	−6	−6	−6	−6	−6	−6	−2	8	−3	−7
g	11	0	-	-	-	-	-	-	-	-	-	-	-	-	-
g	11	1	-	-	-	-	-	-	-	-	-	-	-	-	-
h	11	1	-	-	-	-	-	-	-	-	-	-	-	-	-
g	11	2	-	-	-	-	-	-	-	-	-	-	-	-	-
h	11	2	-	-	-	-	-	-	-	-	-	-	-	-	-
g	11	3	-	-	-	-	-	-	-	-	-	-	-	-	-
h	11	3	-	-	-	-	-	-	-	-	-	-	-	-	-
g	11	4	-	-	-	-	-	-	-	-	-	-	-	-	-
h	11	4	-	-	-	-	-	-	-	-	-	-	-	-	-
g	11	5	-	-	-	-	-	-	-	-	-	-	-	-	-
h	11	5	-	-	-	-	-	-	-	-	-	-	-	-	-
g	11	6	-	-	-	-	-	-	-	-	-	-	-	-	-
h	11	6	-	-	-	-	-	-	-	-	-	-	-	-	-
g	11	7	-	-	-	-	-	-	-	-	-	-	-	-	-
h	11	7	-	-	-	-	-	-	-	-	-	-	-	-	-
g	11	8	-	-	-	-	-	-	-	-	-	-	-	-	-
h	11	8	-	-	-	-	-	-	-	-	-	-	-	-	-
g	11	9	-	-	-	-	-	-	-	-	-	-	-	-	-
h	11	9	-	-	-	-	-	-	-	-	-	-	-	-	-
g	11	10	-	-	-	-	-	-	-	-	-	-	-	-	-
h	11	10	-	-	-	-	-	-	-	-	-	-	-	-	-

Table 2 (continued)

g/h	Deg n	Ord m	IGRF 1900.0	IGRF 1905.0	IGRF 1910.0	IGRF 1915.0	IGRF 1920.0	IGRF 1925.0	IGRF 1930.0	IGRF 1935.0	IGRF 1940.0	DGRF 1945.0	DGRF 1950.0	DGRF 1955.0	DGRF 1960.0
g	11	11	-	-	-	-	-	-	-	-	-	-	-	-	-
h	11	11	-	-	-	-	-	-	-	-	-	-	-	-	-
g	12	0	-	-	-	-	-	-	-	-	-	-	-	-	-
g	12	1	-	-	-	-	-	-	-	-	-	-	-	-	-
h	12	1	-	-	-	-	-	-	-	-	-	-	-	-	-
g	12	2	-	-	-	-	-	-	-	-	-	-	-	-	-
h	12	2	-	-	-	-	-	-	-	-	-	-	-	-	-
g	12	3	-	-	-	-	-	-	-	-	-	-	-	-	-
h	12	3	-	-	-	-	-	-	-	-	-	-	-	-	-
g	12	4	-	-	-	-	-	-	-	-	-	-	-	-	-
h	12	4	-	-	-	-	-	-	-	-	-	-	-	-	-
g	12	5	-	-	-	-	-	-	-	-	-	-	-	-	-
h	12	5	-	-	-	-	-	-	-	-	-	-	-	-	-
g	12	6	-	-	-	-	-	-	-	-	-	-	-	-	-
h	12	6	-	-	-	-	-	-	-	-	-	-	-	-	-
g	12	7	-	-	-	-	-	-	-	-	-	-	-	-	-
h	12	7	-	-	-	-	-	-	-	-	-	-	-	-	-
g	12	8	-	-	-	-	-	-	-	-	-	-	-	-	-
h	12	8	-	-	-	-	-	-	-	-	-	-	-	-	-
g	12	9	-	-	-	-	-	-	-	-	-	-	-	-	-
h	12	9	-	-	-	-	-	-	-	-	-	-	-	-	-
g	12	10	-	-	-	-	-	-	-	-	-	-	-	-	-
h	12	10	-	-	-	-	-	-	-	-	-	-	-	-	-
g	12	11	-	-	-	-	-	-	-	-	-	-	-	-	-
h	12	11	-	-	-	-	-	-	-	-	-	-	-	-	-
g	12	12	-	-	-	-	-	-	-	-	-	-	-	-	-
h	12	12	-	-	-	-	-	-	-	-	-	-	-	-	-
g	13	0	-	-	-	-	-	-	-	-	-	-	-	-	-
g	13	1	-	-	-	-	-	-	-	-	-	-	-	-	-
h	13	1	-	-	-	-	-	-	-	-	-	-	-	-	-
g	13	2	-	-	-	-	-	-	-	-	-	-	-	-	-
h	13	2	-	-	-	-	-	-	-	-	-	-	-	-	-
g	13	3	-	-	-	-	-	-	-	-	-	-	-	-	-
h	13	3	-	-	-	-	-	-	-	-	-	-	-	-	-
g	13	4	-	-	-	-	-	-	-	-	-	-	-	-	-
h	13	4	-	-	-	-	-	-	-	-	-	-	-	-	-

Table 2 (continued)

g/h	Deg n	Ord m	IGRF 1900.0	IGRF 1905.0	IGRF 1910.0	IGRF 1915.0	IGRF 1920.0	IGRF 1925.0	IGRF 1930.0	IGRF 1935.0	IGRF 1940.0	DGRF 1945.0	DGRF 1950.0	DGRF 1955.0	DGRF 1960.0
g	13	5	-	-	-	-	-	-	-	-	-	-	-	-	-
h	13	5	-	-	-	-	-	-	-	-	-	-	-	-	-
g	13	6	-	-	-	-	-	-	-	-	-	-	-	-	-
h	13	6	-	-	-	-	-	-	-	-	-	-	-	-	-
g	13	7	-	-	-	-	-	-	-	-	-	-	-	-	-
h	13	7	-	-	-	-	-	-	-	-	-	-	-	-	-
g	13	8	-	-	-	-	-	-	-	-	-	-	-	-	-
h	13	8	-	-	-	-	-	-	-	-	-	-	-	-	-
g	13	9	-	-	-	-	-	-	-	-	-	-	-	-	-
h	13	9	-	-	-	-	-	-	-	-	-	-	-	-	-
g	13	10	-	-	-	-	-	-	-	-	-	-	-	-	-
h	13	10	-	-	-	-	-	-	-	-	-	-	-	-	-
g	13	11	-	-	-	-	-	-	-	-	-	-	-	-	-
h	13	11	-	-	-	-	-	-	-	-	-	-	-	-	-
g	13	12	-	-	-	-	-	-	-	-	-	-	-	-	-
h	13	12	-	-	-	-	-	-	-	-	-	-	-	-	-
g	13	13	-	-	-	-	-	-	-	-	-	-	-	-	-
h	13	13	-	-	-	-	-	-	-	-	-	-	-	-	-

g/h	Deg n	Ord m	DGRF 1965.0	DGRF 1970.0	DGRF 1975.0	DGRF 1980.0	DGRF 1985.0	DGRF 1990.0	DGRF 1995.0	DGRF 2000.0	DGRF 2005.0	DGRF 2010.0	DGRF 2015.0	IGRF 2020.0	SV 20-25
g	1	0	−30334	−30220	−30100	−29992	−29873	−29775	−29692	−29619.4	−29554.63	−29496.57	−29441.46	−29404.8	5.7
g	1	1	−2119	−2068	−2013	−1956	−1905	−1848	−1784	−1728.2	−1669.05	−1586.42	−1501.77	−1450.9	7.4
h	1	1	5776	5737	5675	5604	5500	5406	5306	5186.1	5077.99	4944.26	4795.99	4652.5	−25.9
g	2	0	−1662	−1781	−1902	−1997	−2072	−2131	−2200	−2267.7	−2337.24	−2396.06	−2445.88	−2499.6	−11.0
g	2	1	2997	3000	3010	3027	3044	3059	3070	3068.4	3047.69	3026.34	3012.20	2982.0	−7.0
h	2	1	−2016	−2047	−2067	−2129	−2197	−2279	−2366	−2481.6	−2594.50	−2708.54	−2845.41	−2991.6	−30.2
g	2	2	1594	1611	1632	1663	1687	1686	1681	1670.9	1657.76	1668.17	1676.35	1677.0	−2.1
h	2	2	114	25	−68	−200	−306	−373	−413	−458.0	−515.43	−575.73	−642.17	−734.6	−22.4
g	3	0	1297	1287	1276	1281	1296	1314	1335	1339.6	1336.30	1339.85	1350.33	1363.2	2.2
g	3	1	−2038	−2091	−2144	−2180	−2208	−2239	−2267	−2288.0	−2305.83	−2326.54	−2352.26	−2381.2	−5.9
h	3	1	−404	−366	−333	−336	−310	−284	−262	−227.6	−198.86	−160.40	−115.29	−82.1	6.0
g	3	2	1292	1278	1260	1251	1247	1248	1249	1252.1	1246.39	1232.10	1225.85	1236.2	3.1
h	3	2	240	251	262	271	284	293	302	293.4	269.72	251.75	245.04	241.9	−1.1
g	3	3	856	838	830	833	829	802	759	714.5	672.51	633.73	581.69	525.7	−12.0
h	3	3	−165	−196	−223	−252	−297	−352	−427	−491.1	−524.72	−537.03	−538.70	−543.4	0.5

Table 2 (continued)

g/h	Deg n	Ord m	DGRF 1965.0	DGRF 1970.0	DGRF 1975.0	DGRF 1980.0	DGRF 1985.0	DGRF 1990.0	DGRF 1995.0	DGRF 2000.0	DGRF 2005.0	DGRF 2010.0	DGRF 2015.0	IGRF 2020.0	SV 20-25
g	4	0	957	952	946	938	936	939	940	932.3	920.55	912.66	907.42	903.0	−1.2
g	4	1	804	800	791	782	780	780	780	786.8	797.96	808.97	813.68	809.5	−1.6
h	4	1	148	167	191	212	232	247	262	272.6	282.07	286.48	283.54	281.9	−0.1
g	4	2	479	461	438	398	361	325	290	250.0	210.65	166.58	120.49	86.3	−5.9
h	4	2	−269	−266	−265	−257	−249	−240	−236	−231.9	−225.23	−211.03	−188.43	−158.4	6.5
g	4	3	−390	−395	−405	−419	−424	−423	−418	−403.0	−379.86	−356.83	−334.85	−309.4	5.2
h	4	3	13	26	39	53	69	84	97	119.8	145.15	164.46	180.95	199.7	3.6
g	4	4	252	234	216	199	170	141	122	111.3	100.00	89.40	70.38	48.0	−5.1
h	4	4	−269	−279	−288	−297	−297	−299	−306	−303.8	−305.36	−309.72	−329.23	−349.7	−5.0
g	5	0	−219	−216	−218	−218	−214	−214	−214	−218.8	−227.00	−230.87	−232.91	−234.3	−0.3
g	5	1	358	359	356	357	355	353	352	351.4	354.41	357.29	360.14	363.2	0.5
h	5	1	19	26	31	46	47	46	46	43.8	42.72	44.58	46.98	47.7	0.0
g	5	2	254	262	264	261	253	245	235	222.3	208.95	200.26	192.35	187.8	−0.6
h	5	2	128	139	148	150	150	154	165	171.9	180.25	189.01	196.98	208.3	2.5
g	5	3	−31	−42	−59	−74	−93	−109	−118	−130.4	−136.54	−141.05	−140.94	−140.7	0.2
h	5	3	−126	−139	−152	−151	−154	−153	−143	−133.1	−123.45	−118.06	−119.14	−121.2	−0.6
g	5	4	−157	−160	−159	−162	−164	−165	−166	−168.6	−168.05	−163.17	−157.40	−151.2	1.3
h	5	4	−97	−91	−83	−78	−75	−69	−55	−39.3	−19.57	−0.01	15.98	32.3	3.0
g	5	5	−62	−56	−49	−48	−46	−36	−17	−12.9	−13.55	−8.03	4.30	13.5	0.9
h	5	5	81	83	88	92	95	97	107	106.3	103.85	101.04	100.12	98.9	0.3
g	6	0	45	43	45	48	53	61	68	72.3	73.60	72.78	69.55	66.0	−0.5
g	6	1	61	64	66	66	65	65	67	68.2	69.56	68.69	67.57	65.5	−0.3
h	6	1	−11	−12	−13	−15	−16	−16	−17	−17.4	−20.33	−20.90	−20.61	−19.1	0.0
g	6	2	8	15	28	42	51	59	68	74.2	76.74	75.92	72.79	72.9	0.4
h	6	2	100	100	99	93	88	82	72	63.7	54.75	44.18	33.30	25.1	−1.6
g	6	3	−228	−212	−198	−192	−185	−178	−170	−160.9	−151.34	−141.40	−129.85	−121.5	1.3
h	6	3	68	72	75	71	69	69	67	65.1	63.63	61.54	58.74	52.8	−1.3
g	6	4	4	2	1	4	4	3	−1	−5.9	−14.58	−22.83	−28.93	−36.2	−1.4
h	6	4	−32	−37	−41	−43	−48	−52	−58	−61.2	−63.53	−66.26	−66.64	−64.5	0.8
g	6	5	1	3	6	14	16	18	19	16.9	14.58	13.10	13.14	13.5	0.0
h	6	5	−8	−6	−4	−2	−1	1	1	0.7	0.24	3.02	7.35	8.9	0.0
g	6	6	−111	−112	−111	−108	−102	−96	−93	−90.4	−86.36	−78.09	−70.85	−64.7	0.9
h	6	6	−7	1	11	17	21	24	36	43.8	50.94	55.40	62.41	68.1	1.0
g	7	0	75	72	71	72	74	77	77	79.0	79.88	80.44	81.29	80.6	−0.1
g	7	1	−57	−57	−56	−59	−62	−64	−72	−74.0	−74.46	−75.00	−75.99	−76.7	−0.2
h	7	1	−61	−70	−77	−82	−83	−80	−69	−64.6	−61.14	−57.80	−54.27	−51.5	0.6

Table 2 (continued)

g/h	Deg n	Ord m	DGRF 1965.0	DGRF 1970.0	DGRF 1975.0	DGRF 1980.0	DGRF 1985.0	DGRF 1990.0	DGRF 1995.0	DGRF 2000.0	DGRF 2005.0	DGRF 2010.0	DGRF 2015.0	IGRF 2020.0	SV 20-25
g	7	2	4	1	1	2	3	2	1	0.0	−1.65	−4.55	−6.79	−8.2	0.0
h	7	2	−27	−27	−26	−27	−27	−26	−25	−24.2	−22.57	−21.20	−19.53	−16.9	0.6
g	7	3	13	14	16	21	24	26	28	33.3	38.73	45.24	51.82	56.5	0.7
h	7	3	−2	−4	−5	−5	−2	0	4	6.2	6.82	6.54	5.59	2.2	−0.8
g	7	4	−26	−22	−14	−12	−6	−1	5	9.1	12.30	14.00	15.07	15.8	0.1
h	7	4	6	8	10	16	20	21	24	24.0	25.35	24.96	24.45	23.5	−0.2
g	7	5	−6	−2	0	1	4	5	4	6.9	9.37	10.46	9.32	6.4	−0.5
h	7	5	26	23	22	18	17	17	17	14.8	10.93	7.03	3.27	−2.2	−1.1
g	7	6	13	13	12	11	10	9	8	7.3	5.42	1.64	−2.88	−7.2	−0.8
h	7	6	−23	−23	−23	−23	−23	−23	−24	−25.4	−26.32	−27.61	−27.50	−27.2	0.1
g	7	7	1	−2	−5	−2	0	0	−2	−1.2	1.94	4.92	6.61	9.8	0.8
h	7	7	−12	−11	−12	−10	−7	−4	−6	−5.8	−4.64	−3.28	−2.32	−1.8	0.3
g	8	0	13	14	14	18	21	23	25	24.4	24.80	24.41	23.98	23.7	0.0
g	8	1	5	6	6	6	6	5	6	6.6	7.62	8.21	8.89	9.7	0.1
h	8	1	7	7	6	7	8	10	11	11.9	11.20	10.84	10.04	8.4	−0.2
g	8	2	−4	−2	−1	0	0	−1	−6	−9.2	−11.73	−14.50	−16.78	−17.6	−0.1
h	8	2	−12	−15	−16	−18	−19	−19	−21	−21.5	−20.88	−20.03	−18.26	−15.3	0.6
g	8	3	−14	−13	−12	−11	−11	−10	−9	−7.9	−6.88	−5.59	−3.16	−0.5	0.4
h	8	3	9	6	4	4	5	6	8	8.5	9.83	11.83	13.18	12.8	−0.2
g	8	4	0	−3	−8	−7	−9	−12	−14	−16.6	−18.11	−19.34	−20.56	−21.1	−0.1
h	8	4	−16	−17	−19	−22	−23	−22	−23	−21.5	−19.71	−17.41	−14.60	−11.7	0.5
g	8	5	8	5	4	4	4	3	9	9.1	10.17	11.61	13.33	15.3	0.4
h	8	5	4	6	6	9	11	12	15	15.5	16.22	16.71	16.16	14.9	−0.3
g	8	6	−1	0	0	3	4	4	6	7.0	9.36	10.85	11.76	13.7	0.3
h	8	6	24	21	18	16	14	12	11	8.9	7.61	6.96	5.69	3.6	−0.4
g	8	7	11	11	10	6	4	2	−5	−7.9	−11.25	−14.05	−15.98	−16.5	−0.1
h	8	7	−3	−6	−10	−13	−15	−16	−16	−14.9	−12.76	−10.74	−9.10	−6.9	0.5
g	8	8	4	3	1	−1	−4	−6	−7	−7.0	−4.87	−3.54	−2.02	−0.3	0.4
h	8	8	−17	−16	−17	−15	−11	−10	−4	−2.1	−0.06	1.64	2.26	2.8	0.0
g	9	0	8	8	7	5	5	4	4	5.0	5.58	5.50	5.33	5.0	–
g	9	1	10	10	10	10	10	9	9	9.4	9.76	9.45	8.83	8.4	–
h	9	1	−22	−21	−21	−21	−21	−20	−20	−19.7	−20.11	−20.54	−21.77	−23.4	–
g	9	2	2	2	2	1	1	1	3	3.0	3.58	3.45	3.02	2.9	–
h	9	2	15	16	16	16	15	15	15	13.4	12.69	11.51	10.76	11.0	–
g	9	3	−13	−12	−12	−12	−12	−12	−10	−8.4	−6.94	−5.27	−3.22	−1.5	–
h	9	3	7	6	7	9	9	11	12	12.5	12.67	12.75	11.74	9.8	–

Table 2 (continued)

g/h	Deg n	Ord m	DGRF 1965.0	DGRF 1970.0	DGRF 1975.0	DGRF 1980.0	DGRF 1985.0	DGRF 1990.0	DGRF 1995.0	DGRF 2000.0	DGRF 2005.0	DGRF 2010.0	DGRF 2015.0	IGRF 2020.0	SV 20-25
g	9	4	10	10	10	9	9	9	8	6.3	5.01	3.13	0.67	−1.1	–
h	9	4	−4	−4	−4	−5	−6	−7	−6	−6.2	−6.72	−7.14	−6.74	−5.1	–
g	9	5	−1	−1	−1	−3	−3	−4	−8	−8.9	−10.76	−12.38	−13.20	−13.2	–
h	9	5	−5	−5	−5	−6	−6	−7	−8	−8.4	−8.16	−7.42	−6.88	−6.3	–
g	9	6	−1	0	−1	−1	−1	−2	−1	−1.5	−1.25	−0.76	−0.10	1.1	–
h	9	6	10	10	10	9	9	9	8	8.4	8.10	7.97	7.79	7.8	–
g	9	7	5	3	4	7	7	7	10	9.3	8.76	8.43	8.68	8.8	–
h	9	7	10	11	11	10	9	8	5	3.8	2.92	2.14	1.04	0.4	–
g	9	8	1	1	1	2	1	1	−2	−4.3	−6.66	−8.42	−9.06	−9.3	–
h	9	8	−4	−2	−3	−6	−7	−7	−8	−8.2	−7.73	−6.08	−3.89	−1.4	–
g	9	9	−2	−1	−2	−5	−5	−6	−8	−8.2	−9.22	−10.08	−10.54	−11.9	–
h	9	9	1	1	1	2	2	2	3	4.8	6.01	7.01	8.44	9.6	–
g	10	0	−2	−3	−3	−4	−4	−3	−3	−2.6	−2.17	−1.94	−2.01	−1.9	–
g	10	1	−3	−3	−3	−4	−4	−4	−6	−6.0	−6.12	−6.24	−6.26	−6.2	–
h	10	1	2	1	1	1	1	2	1	1.7	2.19	2.73	3.28	3.4	–
g	10	2	2	2	2	2	3	2	2	1.7	1.42	0.89	0.17	−0.1	–
h	10	2	1	1	1	0	0	1	0	0.0	0.10	−0.10	−0.40	−0.2	–
g	10	3	−5	−5	−5	−5	−5	−5	−4	−3.1	−2.35	−1.07	0.55	1.7	–
h	10	3	2	3	3	3	3	3	4	4.0	4.46	4.71	4.55	3.6	–
g	10	4	−2	−1	−2	−2	−2	−2	−1	−0.5	−0.15	−0.16	−0.55	−0.9	–
h	10	4	6	4	4	6	6	6	5	4.9	4.76	4.44	4.40	4.8	–
g	10	5	4	6	5	5	5	4	4	3.7	3.06	2.45	1.70	0.7	–
h	10	5	−4	−4	−4	−4	−4	−4	−5	−5.9	−6.58	−7.22	−7.92	−8.6	–
g	10	6	4	4	4	3	3	3	2	1.0	0.29	−0.33	−0.67	−0.9	–
h	10	6	0	0	−1	0	0	0	−1	−1.2	−1.01	−0.96	−0.61	−0.1	–
g	10	7	0	1	1	1	1	1	2	2.0	2.06	2.13	2.13	1.9	–
h	10	7	−2	−1	−1	−1	−1	−2	−2	−2.9	−3.47	−3.95	−4.16	−4.3	–
g	10	8	2	0	0	2	2	3	5	4.2	3.77	3.09	2.33	1.4	–
h	10	8	3	3	3	4	4	3	1	0.2	−0.86	−1.99	−2.85	−3.4	–
g	10	9	2	3	3	3	3	3	1	0.3	−0.21	−1.03	−1.80	−2.4	–
h	10	9	0	1	1	0	0	−1	−2	−2.2	−2.31	−1.97	−1.12	−0.1	–
g	10	10	0	−1	−1	0	0	0	0	−1.1	−2.09	−2.80	−3.59	−3.8	–
h	10	10	−6	−4	−5	−6	−6	−6	−7	−7.4	−7.93	−8.31	−8.72	−8.8	–
g	11	0	-	-	-	-	-	-	-	2.7	2.95	3.05	3.00	3.0	–
g	11	1	-	-	-	-	-	-	-	−1.7	−1.60	−1.48	−1.40	−1.4	–

Table 2 (continued)

g/h	Deg n	Ord m	DGRF 1965.0	DGRF 1970.0	DGRF 1975.0	DGRF 1980.0	DGRF 1985.0	DGRF 1990.0	DGRF 1995.0	DGRF 2000.0	DGRF 2005.0	DGRF 2010.0	DGRF 2015.0	IGRF 2020.0	SV 20-25
h	11	1	-	-	-	-	-	-	-	0.1	0.26	0.13	0.00	0.0	–
g	11	2	-	-	-	-	-	-	-	−1.9	−1.88	−2.03	−2.30	−2.5	–
h	11	2	-	-	-	-	-	-	-	1.3	1.44	1.67	2.11	2.5	–
g	11	3	-	-	-	-	-	-	-	1.5	1.44	1.65	2.08	2.3	–
h	11	3	-	-	-	-	-	-	-	−0.9	−0.77	−0.66	−0.60	−0.6	–
g	11	4	-	-	-	-	-	-	-	−0.1	−0.31	−0.51	−0.79	−0.9	–
h	11	4	-	-	-	-	-	-	-	−2.6	−2.27	−1.76	−1.05	−0.4	–
g	11	5	-	-	-	-	-	-	-	0.1	0.29	0.54	0.58	0.3	–
h	11	5	-	-	-	-	-	-	-	0.9	0.90	0.85	0.76	0.6	–
g	11	6	-	-	-	-	-	-	-	−0.7	−0.79	−0.79	−0.70	−0.7	–
h	11	6	-	-	-	-	-	-	-	−0.7	−0.58	−0.39	−0.20	−0.2	–
g	11	7	-	-	-	-	-	-	-	0.7	0.53	0.37	0.14	−0.1	–
h	11	7	-	-	-	-	-	-	-	−2.8	−2.69	−2.51	−2.12	−1.7	–
g	11	8	-	-	-	-	-	-	-	1.7	1.80	1.79	1.70	1.4	–
h	11	8	-	-	-	-	-	-	-	−0.9	−1.08	−1.27	−1.44	−1.6	–
g	11	9	-	-	-	-	-	-	-	0.1	0.16	0.12	−0.22	−0.6	–
h	11	9	-	-	-	-	-	-	-	−1.2	−1.58	−2.11	−2.57	−3.0	–
g	11	10	-	-	-	-	-	-	-	1.2	0.96	0.75	0.44	0.2	–
h	11	10	-	-	-	-	-	-	-	−1.9	−1.90	−1.94	−2.01	−2.0	–
g	11	11	-	-	-	-	-	-	-	4.0	3.99	3.75	3.49	3.1	–
h	11	11	-	-	-	-	-	-	-	−0.9	−1.39	−1.86	−2.34	−2.6	–
g	12	0	-	-	-	-	-	-	-	−2.2	−2.15	−2.12	−2.09	−2.0	–
g	12	1	-	-	-	-	-	-	-	−0.3	−0.29	−0.21	−0.16	−0.1	–
h	12	1	-	-	-	-	-	-	-	−0.4	−0.55	−0.87	−1.08	−1.2	–
g	12	2	-	-	-	-	-	-	-	0.2	0.21	0.30	0.46	0.5	–
h	12	2	-	-	-	-	-	-	-	0.3	0.23	0.27	0.37	0.5	–
g	12	3	-	-	-	-	-	-	-	0.9	0.89	1.04	1.23	1.3	–
h	12	3	-	-	-	-	-	-	-	2.5	2.38	2.13	1.75	1.4	–
g	12	4	-	-	-	-	-	-	-	−0.2	−0.38	−0.63	−0.89	−1.2	–
h	12	4	-	-	-	-	-	-	-	−2.6	−2.63	−2.49	−2.19	−1.8	–
g	12	5	-	-	-	-	-	-	-	0.9	0.96	0.95	0.85	0.7	–
h	12	5	-	-	-	-	-	-	-	0.7	0.61	0.49	0.27	0.1	–
g	12	6	-	-	-	-	-	-	-	−0.5	−0.30	−0.11	0.10	0.3	–
h	12	6	-	-	-	-	-	-	-	0.3	0.40	0.59	0.72	0.8	–
g	12	7	-	-	-	-	-	-	-	0.3	0.46	0.52	0.54	0.5	–

Table 2 (continued)

g/h	Deg n	Ord m	DGRF 1965.0	DGRF 1970.0	DGRF 1975.0	DGRF 1980.0	DGRF 1985.0	DGRF 1990.0	DGRF 1995.0	DGRF 2000.0	DGRF 2005.0	DGRF 2010.0	DGRF 2015.0	IGRF 2020.0	SV 20-25
h	12	7	-	-	-	-	-	-	-	0.0	0.01	0.00	−0.09	−0.2	–
g	12	8	-	-	-	-	-	-	-	−0.3	−0.35	−0.39	−0.37	−0.3	–
h	12	8	-	-	-	-	-	-	-	0.0	0.02	0.13	0.29	0.6	–
g	12	9	-	-	-	-	-	-	-	−0.4	−0.36	−0.37	−0.43	−0.5	–
h	12	9	-	-	-	-	-	-	-	0.3	0.28	0.27	0.23	0.2	–
g	12	10	-	-	-	-	-	-	-	−0.1	0.08	0.21	0.22	0.1	–
h	12	10	-	-	-	-	-	-	-	−0.9	−0.87	−0.86	−0.89	−0.9	–
g	12	11	-	-	-	-	-	-	-	−0.2	−0.49	−0.77	−0.94	−1.1	–
h	12	11	-	-	-	-	-	-	-	−0.4	−0.34	−0.23	−0.16	0.0	–
g	12	12	-	-	-	-	-	-	-	−0.4	−0.08	0.04	−0.03	−0.3	–
h	12	12	-	-	-	-	-	-	-	0.8	0.88	0.87	0.72	0.5	–
g	13	0	-	-	-	-	-	-	-	−0.2	−0.16	−0.09	−0.02	0.1	–
g	13	1	-	-	-	-	-	-	-	−0.9	−0.88	−0.89	−0.92	−0.9	–
h	13	1	-	-	-	-	-	-	-	−0.9	−0.76	−0.87	−0.88	−0.9	–
g	13	2	-	-	-	-	-	-	-	0.3	0.30	0.31	0.42	0.5	–
h	13	2	-	-	-	-	-	-	-	0.2	0.33	0.30	0.49	0.6	–
g	13	3	-	-	-	-	-	-	-	0.1	0.28	0.42	0.63	0.7	–
h	13	3	-	-	-	-	-	-	-	1.8	1.72	1.66	1.56	1.4	–
g	13	4	-	-	-	-	-	-	-	−0.4	−0.43	−0.45	−0.42	−0.3	–
h	13	4	-	-	-	-	-	-	-	−0.4	−0.54	−0.59	−0.50	−0.4	–
g	13	5	-	-	-	-	-	-	-	1.3	1.18	1.08	0.96	0.8	–
h	13	5	-	-	-	-	-	-	-	−1.0	−1.07	−1.14	−1.24	−1.3	–
g	13	6	-	-	-	-	-	-	-	−0.4	−0.37	−0.31	−0.19	0.0	–
h	13	6	-	-	-	-	-	-	-	−0.1	−0.04	−0.07	−0.10	−0.1	–
g	13	7	-	-	-	-	-	-	-	0.7	0.75	0.78	0.81	0.8	–
h	13	7	-	-	-	-	-	-	-	0.7	0.63	0.54	0.42	0.3	–
g	13	8	-	-	-	-	-	-	-	−0.4	−0.26	−0.18	−0.13	0.0	–
h	13	8	-	-	-	-	-	-	-	0.3	0.21	0.10	−0.04	−0.1	–
g	13	9	-	-	-	-	-	-	-	0.3	0.35	0.38	0.38	0.4	–
h	13	9	-	-	-	-	-	-	-	0.6	0.53	0.49	0.48	0.5	–
g	13	10	-	-	-	-	-	-	-	−0.1	−0.05	0.02	0.08	0.1	–
h	13	10	-	-	-	-	-	-	-	0.3	0.38	0.44	0.48	0.5	–
g	13	11	-	-	-	-	-	-	-	0.4	0.41	0.42	0.46	0.5	–
h	13	11	-	-	-	-	-	-	-	−0.2	−0.22	−0.25	−0.30	−0.4	–

Table 2 (continued)

g/h	Deg	Ord	DGRF	DGRF	DGRF	DGRF	DGRF	DGRF	DGRF	DGRF	DGRF	DGRF	DGRF	IGRF	SV
	n	m	1965.0	1970.0	1975.0	1980.0	1985.0	1990.0	1995.0	2000.0	2005.0	2010.0	2015.0	2020.0	20-25
g	13	12	-	-	-	-	-	-	-	0.0	−0.10	−0.26	−0.35	−0.5	–
h	13	12	-	-	-	-	-	-	-	−0.5	−0.57	−0.53	−0.43	−0.4	–
g	13	13	-	-	-	-	-	-	-	0.1	−0.18	−0.26	−0.36	−0.4	–
h	13	13	-	-	-	-	-	-	-	−0.9	−0.82	−0.79	−0.71	−0.6	–

This table provides Schmidt-normalized spherical harmonic coefficients. Coefficients for degrees n=1-13 in units of nT are listed for IGRF and definitive DGRF main field models. Coefficients for degrees n=1-8 in units of nT/year are listed for the predictive secular variation. Undefined coefficients are marked with '-'; these should be set to 0.0 in numerical calculations as is the case in the coefficient file available online

$\dot{g}_n^m(T_t), \dot{h}_n^m(T_t)$ represent the linear approximation to the change in the Gauss coefficients over the 5-year interval spanning $[T_t, T_t + 5]$. They may be computed in units of nanoTesla per year (nT/year) as

$$\dot{g}_n^m(T_t) = \frac{1}{5}\left(g_n^m(T_t + 5) - g_n^m(T_t)\right), \tag{4}$$

$$\dot{h}_n^m(T_t) = \frac{1}{5}\left(h_n^m(T_t + 5) - h_n^m(T_t)\right). \tag{5}$$

The main field coefficients are not yet known for $T_t = 2025$, and so for the final 5 years of model validity (2020 to 2025 for IGRF-13), the coefficients $\dot{g}_n^m(2020), \dot{h}_n^m(2020)$ are explicitly provided (see last column of Table 2) in units of nT/year. Details on the individual candidate secular variation forecasts and the procedure used to combine them into a final set of $\dot{g}_n^m(2020), \dot{h}_n^m(2020)$ may be found in Alken et al. (2020b) and references therein.

The 13th generation IGRF

In August 2017, during an IAGA V-MOD Working Group meeting held in Cape Town, South Africa, a task force of volunteer geomagnetic modelers was assembled to oversee the call for IGRF-13 candidate models and their evaluation. In March 2019, the task force issued an international call for three candidates:

- A DGRF main field model for the epoch 2015.0
- An IGRF main field model for the epoch 2020.0
- An IGRF linear secular variation model for the time period 2020.0 to 2025.0.

Fifteen teams representing over 30 international institutes responded to the call. The number of teams and institutions who participated in IGRF-13 exceeded that of any previous generation. The task force received 11 DGRF main field candidates for epoch 2015.0, 12 IGRF main field candidates for 2020.0, and 14 IGRF secular variation candidates for 2020.0-2025.0. Following recent IGRF conventions, the main field candidates for IGRF-13 describe the spatial variation of the field to a maximum spherical harmonic degree and order of 13, while the secular variation candidates extend to a maximum degree and order of 8. Each of the 15 teams was managed by a team leader from the *lead institution*, and many teams also included personnel from supporting institutions. The 15 lead institutions for IGRF-13, including references to their candidate model papers, are: (1) British Geological Survey (UK) (Brown et al. 2020); (2) Institute of Crustal Dynamics, China Earthquake Administration (China) (Yang et al. 2020); (3) Universidad Complutense de

Madrid (Spain) (Pavón-Carrasco et al. 2020); (4) University of Colorado Boulder (USA) (Alken et al. 2020a); (5) Technical University of Denmark (Denmark) (Finlay et al. 2020); (6) GFZ German Research Centre for Geosciences (Germany) (Rother et al. 2020); (7) Institut de physique du globe de Paris (France) (Fournier et al. 2020; Vigneron et al. 2020; Ropp et al. 2020); (8) Institut des Sciences de la Terre (France) (Huder et al. 2020); (9) Pushkov Institute of Terrestrial Magnetism, Ionosphere and Radio Wave Propagation (Russia) (Petrov and Bondar 2020); (10) Kyoto University (Japan) (Minami et al. 2020); (11) University of Leeds (UK) (Metman et al. 2020); (12) Max Planck Institute for Solar System Research (Germany) (Sanchez et al. 2020); (13) NASA Goddard Space Flight Center (USA) (Sabaka et al. 2020; Tangborn et al. 2020); (14) University of Potsdam (Germany) (Baerenzung et al. 2020), and (15) Université de Strasbourg (France) (Wardinski et al. 2020). Some of the lead institutes listed above also acted as supporting institutions to other teams. The supporting institutes which are not listed above include: Geoscience Institute (Spain), Hebei GEO University (China), Institute of Earthquake Forecasting, China Earthquake Administration (China), Institute of Geophysics, China Earthquake Administration (China), Kyushu University (Japan), Nagoya University (Japan), National Space Science Center, Chinese Academy of Sciences (China), Observatori de l'Ebre (Spain), Observatorio Geofísico de Toledo (Spain), Real Observatorio Geofísico de la Armada (Spain), Space Research Institute of the Austrian Academy of Sciences (Austria), The Institute of Statistical Mathematics (Japan), Tokyo Institute of Technology (Japan), Université de Nantes (France), and University of Tokyo (Japan).

Data recorded by the Swarm satellite mission (Friis-Christensen et al. 2006) and the ground observatory network (see Table 3) played a crucial role in the development of many of the IGRF-13 candidate models. Data from the Ørsted (Olsen et al. 2000), CHAMP (Reigber et al. 2002), SAC-C (Colomb et al. 2004), Cryosat-2, and CSES (Shen et al. 2018) missions were also used by some of the teams. The IGRF-13 task force voted to calculate the final main field models for epochs 2015.0 and 2020.0 as the medians of the Gauss coefficients of all the candidate models. The task force voted to use a robust Huber weighting in space to determine the final secular variation model for 2020.0 to 2025.0. Further details of the candidate models, the evaluation process, and the final model determination are provided in Alken et al. (2020b).

IGRF-13 model coefficients and maps

Table 2 lists the IGRF-13 spherical harmonic Gauss coefficients, which can be used with Eq. (1) to determine the geomagnetic potential (and vector geomagnetic field) anywhere on or above Earth's surface. This table serves as a published record of IGRF-13, which should allow users to ensure they use the correct model coefficients for a particular epoch compared with previous generations. The main field coefficients are given in units of nT, and the predictive secular variation coefficients (last column) are given in units of nT/year. These coefficients are available in digital form from https://www.ngdc.noaa.gov/IAGA/vmod/igrf.html along with software to compute magnetic field components at different times and spatial locations, in both geocentric and geodetic coordinate systems.

Figure 1 shows global maps of the IGRF-13 declination (D), inclination (I), and total field magnitude (F) on Earth's surface at 2020 in Miller cylindrical projection. Taken together, these three quantities fully describe the vector magnetic field at Earth's surface. The green contour lines represent zero. For the declination component (top panel), these are the agonic lines on which a magnetic compass needle would point to true geographic north. For the inclination map (middle panel), the green contour line of zero inclination shows the magnetic dip equator, which approximately aligns with the geographic equator except for a large, well-known southward deviation over South America. The F map (bottom panel) shows that the largest field intensities occur in Siberia in the northern hemisphere and in the Southern Ocean between Australia and Antarctic in the southern hemisphere. We also see a region of significantly weaker field (compared to an idealized dipole), centered over South America, which is known as the South Atlantic Anomaly. In this region, the inner Van Allen radiation belt comes closest to Earth's surface, which has important consequences for satellite instrumentation and human safety in low Earth orbit. Interestingly, a new second minimum is becoming more pronounced over the southern Atlantic. This feature is described in more detail in Rother et al. (2020) and Finlay et al. (2020) and was earlier reported by Terra-Nova et al. (2019).

Figure 2 shows the predicted average change of the D, I, and F components on Earth's surface during the 2020 to 2025 interval from IGRF-13. At low and middle latitudes, the map of dD/dt (top panel) predicts the largest declination changes in the South Atlantic Anomaly region and also in the polar regions, with northern polar declination changing more than in the southern polar region. The dI/dt map (middle panel) predicts the largest changes over Brazil, where the magnetic dip equator has moved relatively rapidly over the past few decades. The features seen in dF/dt (bottom panel) near South America predict a deepening and westward movement of the South Atlantic Anomaly, continuing a trend observed over the past century (Finlay et al. 2010a, Fig. 3).

Table 3 Magnetic observatories contributing data used in the construction of IGRF-13

Supporting agencies	Country	Observatory IAGA code
Centre de Recherche en Astronomie, Astrophysique et Geophysique	Algeria	TAM
Universidad Nacional de la Plata	Argentina	TRW
Servicio Meteorologico Nacional	Argentina	PIL, ORC
Geoscience Australia	Australia	ASP, CKI, CNB, CSY, CTA, DVS
		GNA, GNG, KDU, LRM, MAW, MCQ
Zentralanstalt für Meteorologie und Geodynamik	Austria	WIC
National Academy of Sciences	Belarus	MNK
Institut Royal Météorologique	Belgium	DOU, MAB
CNPq-Observatorio Nacional	Brazil	VSS, TTB
Academy of Sciences	Bulgaria	PAG
Geological Survey of Canada	Canada	ALE, BLC, BRD, CBB, FCC, IQA
		MEA, OTT, RES, STJ, VIC,YKC
Centro Meteorológico Regional Pacifico	Chile	IPM
Academy of Sciences	China	BMT, SSH
China Earthquake Administration	China	CDP, CNH, GLM, GZH, KSH, LZH
		MZL, QGZ, QIX, QZH, THJ, WHN
Instituto Geographico Agustin Codazzi	Columbia	FUQ
University of Zagreb	Croatia	LON
Academy of Sciences	Czech Republic	BDV
Technical University of Denmark, DTU Space	Denmark	BFE, NAQ, GDH, THL
Addis Ababa University	Ethiopia	AAE
Finnish Meteorological Institute	Finland	NUR
Geophysical Observatory	Finland	SOD
Institut de Physique du Globe de Paris	France	AAE, BOX, CLF, DLT, KOU, IPM
		LZH, MBO, PHU, PPT, TAM
Ecole et Observatoire des Sciences de la Terre	France	AMS, CZT, DMC, DRV, PAF, TAN
Institut de recherche pour le développement	France	BNG, MBO
Georgian Academy of Sciences	Georgia	TFS
Universität München	Germany	FUR
Alfred-Wegener-Institute for Polar Marine Research	Germany	VNA
GFZ German Research Centre for Geosciences	Germany	ABG, BFO, GAN, HYD, KMH, MGD, NGK, PAG
		PET, SHE, SUA, TDC, TTB, VNA, VSS, WNG, YAK
Universität Stuttgart and KIT	Germany	BFO
Institute of Geology and Mineral Exploration	Greece	PEG
Academy of Sciences	Hungary	NCK
Mining and Geological Survey of Hungary	Hungary	THY
University of Iceland	Iceland	LRV
Indian Institute of Geomagnetism	India	ABG, JAI, NGP, PND, SIL
		SHL, TIR, UJJ, VSK
National Geophysical Research Institute	India	HYB
Meteorological and Geophysical Agency	Indonesia	KPG, PLR, TND, TUN
Meteorological Service	Ireland	VAL
Survey of Israel	Israel	AMT, BGY, ELT
Instituto Nazionale di Geofisica e Vulcanologia	Italy	AQU, CTS, DMC
Japan Coast Guard	Japan	HTY
Japan Meteorological Agency	Japan	CBI, KAK, KNY, MMB
Geographical Survey Institute	Japan	ESA, KNZ, MIZ
Institute of the Ionosphere	Kazakhstan	AAA
Korean Meteorological Administration	Rep of Korea	CYG

Table 3 (continued)

Supporting agencies	Country	Observatory IAGA code
Institut et Observatoire Géophysique d'Antananarivo	Madagascar	TAN
Gan Meteorological Office	Maldives	GAN
Direção Provincial de Recursos Minerais e Energia de Tete	Mozambique	LMM, NMP
Instituto de Geofisica de UNAM	Mexico	TEO
Institute of Geological and Nuclear Sciences	New Zealand	API, EYR, SBA
University of Tromsø	Norway	BJN, DOB, TRO
Instituto Geofisico del Peru	Peru	HUA
Academy of Sciences	Poland	BEL, HLP, HRN
Universidade de Coimbra	Portugal	COI
Geological Survey of Romania	Romania	SUA
AARI	Russia	VOS
GC RAS	Russia	ARS, BOX, SPG
IG UB RAS	Russia	ARS
IKIR-RAS	Russia	KHB, MGD, PET
IPGG SB RAS	Russia	NVS
ISTP SB RAS	Russia	IRT
SHICRA SB RAS	Russia	YAK
Dept. of Agriculture, Forestry, Fisheries & Meteorology	Samoa	API
Geomagnetic College Grocka	Serbia & Montenegro	GCK
Slovenska Akademia Vied	Slovakia	HRB
National Research Foundation	South Africa	HBK, HER, KMH, TSU
Observatori de l'Ebre	Spain	EBR, LIV
Real Instituto y Observatorio de la Armada	Spain	SFS
Instituto Geográfico Nacional	Spain	GUI, SPT
Sveriges Geologiska Undersökning	Sweden	ABK, LYC, UPS
Swedish Institute of Space Physics	Sweden	KIR
ETH Zurich	Switzerland	GAN
Bǒgaziçi University	Turkey	IZN
Academy of Sciences	Ukraine	AIA, LVV, KIV
British Geological Survey	United Kingdom	ASC, ESK, HAD, JCO, KEP, LER, PST, SBL
US Geological Survey	United States	BRW, BOU, BSL, CMO, DED, FRD, FRN
		GUA, HON, NEW, SIT, SJG, SHU, TUC
Academy of Science and Technology	Vietnam	DLT, PHU

Figure 3 presents the positions of the geomagnetic poles and dip poles as given by IGRF-13 for 1900 to 2020, and the predicted positions in 2025. The geomagnetic poles are calculated from the three dipole ($n = 1$) Gauss coefficients and correspond to where the magnetic dipole axis intersects a sphere of mean Earth radius 6371.2 km. These poles are antipodal and are also known as *centered dipole* poles (Laundal and Richmond 2017, Eq. 14). The geomagnetic poles can be used to specify the relative orientation of Earth's magnetic field with respect to the Sun, and they are often used in magnetospheric studies for this purpose. The magnetic dip poles are defined as the locations where the main magnetic field as a whole is normal to Earth's surface, represented by the WGS84 reference ellipsoid. Equivalently, they can be defined as the locations where the magnetic field component tangent to the ellipsoid vanishes. Here, we use the full set of IGRF-13 coefficients to spherical harmonic degree N. Magnetic dip poles provide a key reference for local orientation when navigating on or close to Earth's surface at high-latitudes. For a perfect dipole field, the geomagnetic and dip poles would nearly coincide, but not exactly since the geomagnetic poles are defined with respect to a sphere of mean Earth radius, while the dip poles are defined with respect to the WGS84 ellipsoid. However, as can be seen in the figure, there are significant differences between the two due to the non-dipolar structure

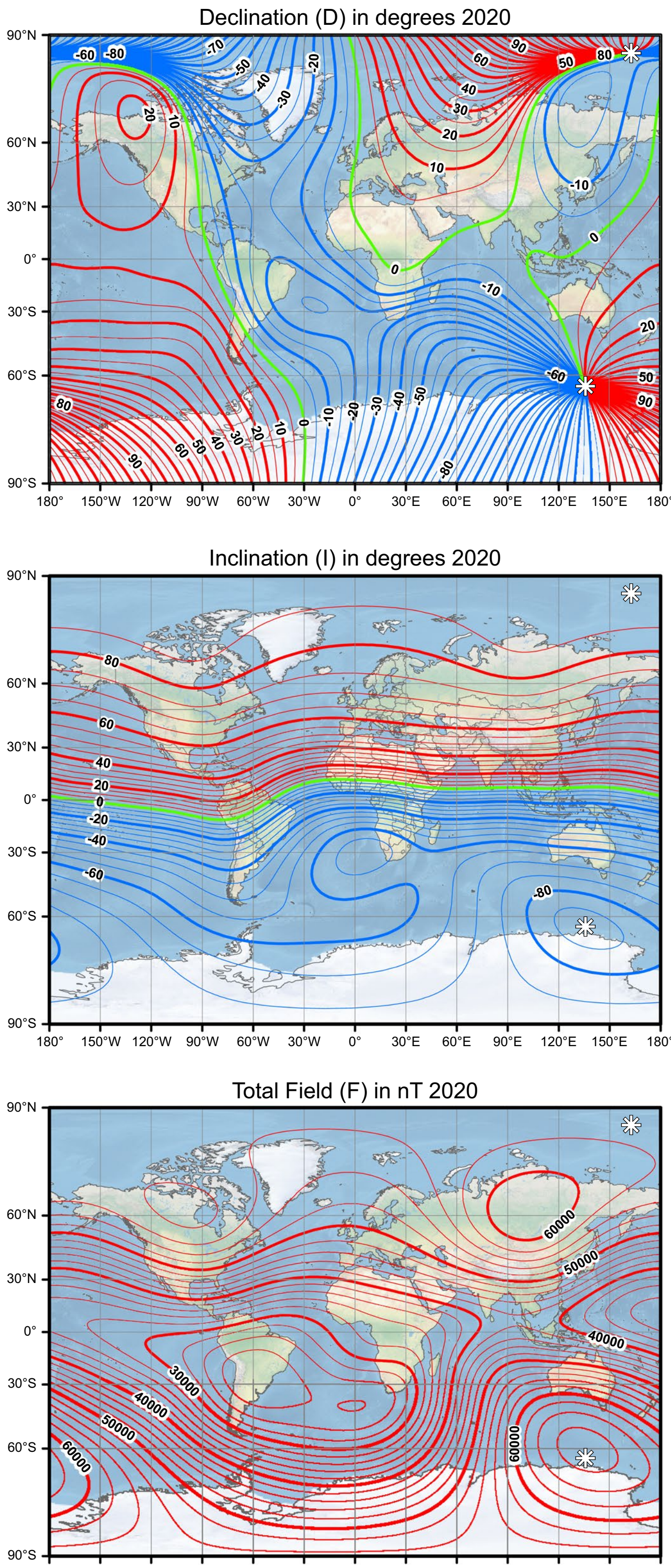

Fig. 1 Maps of declination (top), inclination (middle) and total field (bottom) at the WGS84 ellipsoid surface for epoch 2020. The zero contour is shown in green, positive contours in red, and negative contours in blue. White asterisks indicate locations of the magnetic dip poles. Projection is Miller cylindrical

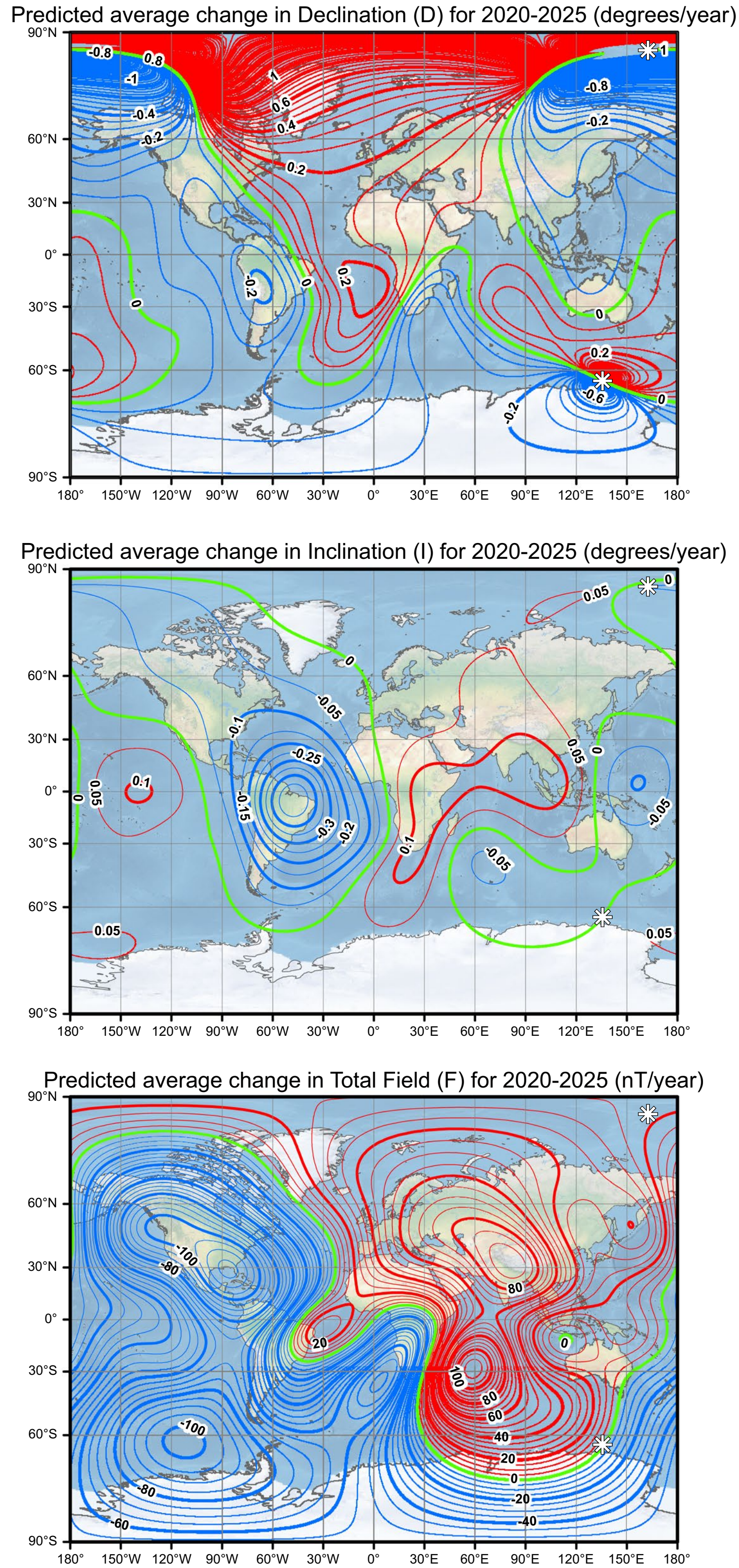

Fig. 2 Maps of predicted annual secular variation in declination (top), inclination (middle) and total field (bottom) at the WGS84 ellipsoid surface averaged over 2020 to 2025. The zero contour is shown in green, positive contours in red, and negative contours in blue. White asterisks indicate locations of the magnetic dip poles. Projection is Miller cylindrical

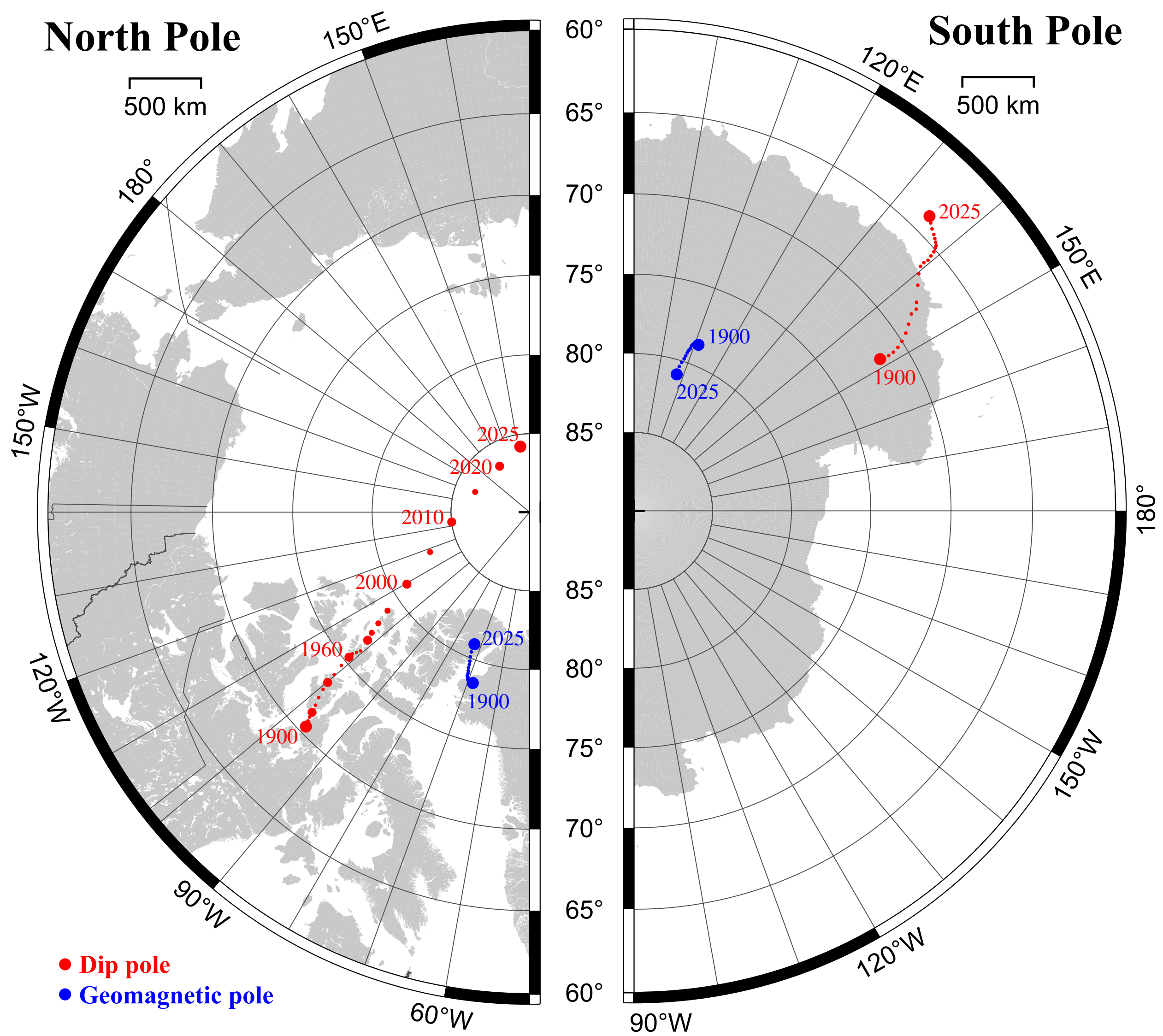

Fig. 3 Motion of the magnetic dip pole (red) and geomagnetic pole (blue) since 1900 from IGRF-13 in the northern hemisphere (left) and southern hemisphere (right). The scale provides an indication of distance on the WGS84 ellipsoid that is correct along lines of constant longitude and also along the middle lines of latitude shown. Note the left and right panels use different longitude ranges. The maps use stereographic projection. International and provincial boundaries are drawn in the left panel

of Earth's magnetic field. The geomagnetic and dip pole locations are provided in Table 4.

Figure 4 shows the speed of the two magnetic dip poles. The north magnetic dip pole experienced a strong acceleration from about 1960 to 2000, but has seen a modest deceleration over the past 20 years, peaking at 55.8 km/year in 2002.5 and slowing slightly to 50.6 km/year in 2017.5. IGRF-13 forecasts a speed of 39.8 km/year in 2022.5, however we caution that past IGRF forecasts contained significant errors (Finlay et al. 2010b). As an example, IGRF-12 predicted a north dip pole speed of 42.6 km/year for 2017.5 (Thébault et al. 2015), compared with the IGRF-13 value of 50.6 km/year. Uncertainties present in IGRF models are further discussed by Lowes (2000).

At Earth's surface in 2020, the contribution from the dipole terms g_1^0, g_1^1, h_1^1 accounts for over 93% of the power in the main geomagnetic field. It is therefore instructive to monitor the temporal change in the dipole moment, which is defined as:

Table 4 Magnetic pole position since 1900 determined from IGRF-13 in units of degrees. Latitudes are provided in the WGS84 geodetic system

Epoch	North dip pole		South dip pole		North geomagnetic pole		South geomagnetic pole	
	Latitude	Longitude	Latitude	Longitude	Latitude	Longitude	Latitude	Longitude
1900.0	70.46	−96.19	−71.72	148.32	78.68	−68.79	−78.68	111.21
1905.0	70.66	−96.48	−71.46	148.54	78.68	−68.75	−78.68	111.25
1910.0	70.79	−96.72	−71.15	148.64	78.66	−68.72	−78.66	111.28
1915.0	71.03	−97.03	−70.80	148.54	78.64	−68.57	−78.64	111.43
1920.0	71.34	−97.38	−70.41	148.20	78.63	−68.38	−78.63	111.62
1925.0	71.79	−97.99	−69.99	147.62	78.62	−68.27	−78.62	111.73
1930.0	72.27	−98.68	−69.52	146.79	78.60	−68.26	−78.60	111.74
1935.0	72.80	−99.33	−69.06	145.76	78.57	−68.36	−78.57	111.64
1940.0	73.30	−99.87	−68.57	144.59	78.55	−68.51	−78.55	111.49
1945.0	73.93	−100.24	−68.15	144.44	78.55	−68.53	−78.55	111.47
1950.0	74.64	−100.86	−67.89	143.55	78.55	−68.85	−78.55	111.15
1955.0	75.18	−101.42	−67.19	141.50	78.54	−69.16	−78.54	110.84
1960.0	75.30	−101.03	−66.70	140.23	78.58	−69.47	−78.58	110.53
1965.0	75.63	−101.34	−66.33	139.53	78.60	−69.85	−78.60	110.15
1970.0	75.88	−100.97	−66.02	139.40	78.66	−70.18	−78.66	109.82
1975.0	76.15	−100.64	−65.74	139.52	78.76	−70.47	−78.76	109.53
1980.0	76.91	−101.68	−65.42	139.35	78.88	−70.76	−78.88	109.24
1985.0	77.40	−102.61	−65.13	139.18	79.04	−70.90	−79.04	109.10
1990.0	78.10	−103.69	−64.91	138.90	79.21	−71.13	−79.21	108.87
1995.0	79.04	−105.29	−64.79	138.73	79.39	−71.42	−79.39	108.58
2000.0	80.97	−109.64	−64.66	138.30	79.61	−71.57	−79.61	108.43
2005.0	83.19	−118.22	−64.55	137.85	79.82	−71.81	−79.82	108.19
2010.0	85.02	−132.84	−64.43	137.32	80.09	−72.21	−80.09	107.79
2015.0	86.31	−160.34	−64.28	136.60	80.38	−72.61	−80.38	107.39
2020.0	86.49	162.87	−64.08	135.87	80.65	−72.68	−80.65	107.32
2025.0	85.78	138.06	−63.85	135.06	80.90	−72.64	−80.90	107.36

$$M(t) = \frac{4\pi}{\mu_0} a^3 \sqrt{g_1^0(t)^2 + g_1^1(t)^2 + h_1^1(t)^2}. \tag{6}$$

Figure 5 presents the change in the dipole moment of the geomagnetic field since 1900 as predicted by IGRF-13 (red). We see a clear downward trend in the dipole strength since the beginning of the last century, which is continued in 2020 and also in the forecast for 2025. This steady downward trend extends back at least as far as 1600 (Merrill et al. 1996; Constable and Korte 2015), although archeomagnetic and paleomagnetic records have revealed much lower dipole moments thousands of years in the past (Panovska et al. 2019). Due to sparsity of data, archeomagnetic and paleomagnetic studies often estimate the dipole strength along the rotation axis, ignoring the off-axis terms g_1^1, h_1^1. This so-called axial dipole moment is defined as $M_A(t) = 4\pi a^3 |g_1^0(t)|/\mu_0$ and is shown in blue in the figure.

IGRF-13 online data products

Further general information about IGRF: https://www.ngdc.noaa.gov/IAGA/vmod/igrf.html

Coefficients of IGRF-13 in ASCII format: https://www.ngdc.noaa.gov/IAGA/vmod/coeffs/igrf13coeffs.txt

Fortran software to compute magnetic field components from coefficients: https://www.ngdc.noaa.gov/IAGA/vmod/igrf13.f

Linux C software to compute magnetic field components from coefficients: https://www.ngdc.noaa.gov/IAGA/vmod/geomag70_linux.tar.gz

Windows C software to compute magnetic field components from coefficients: https://www.ngdc.noaa.gov/IAGA/vmod/geomag70_windows.zip

Python software to compute magnetic field components from coefficients: https://www.ngdc.noaa.gov/IAGA/vmod/pyIGRF.zip

Online calculation of magnetic field components for IGRF-13: https://www.ngdc.noaa.gov/geomag/calculators/magcalc.shtml and http://geomag.bgs.ac.uk/data_servi

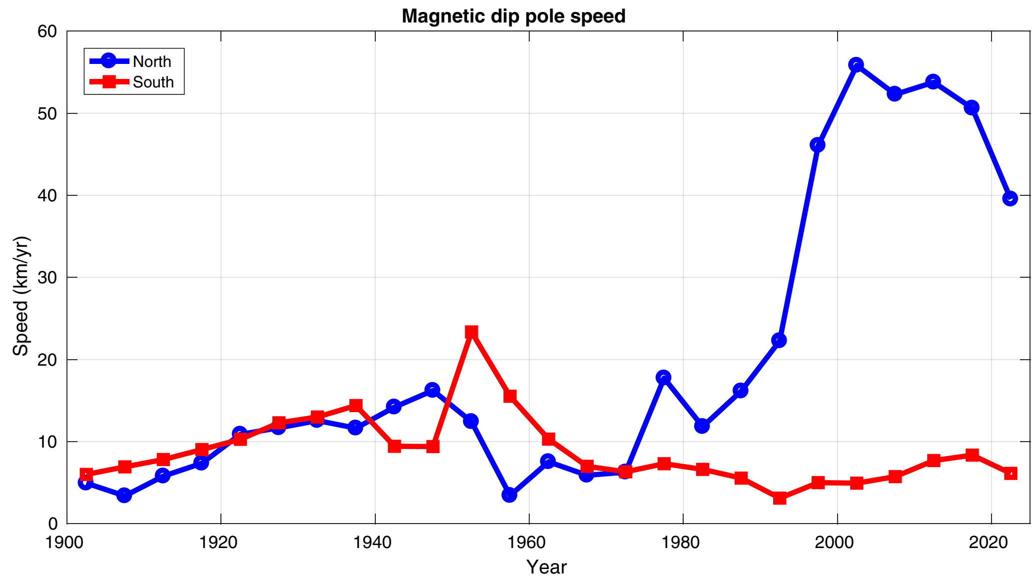

Fig. 4 Average speed of the magnetic dip poles over each 5-year epoch, plotted at the midpoint between epochs (i.e., the speed over 2015–2020 is shown at 2017.5). The value for 2020–2025 is a forecast

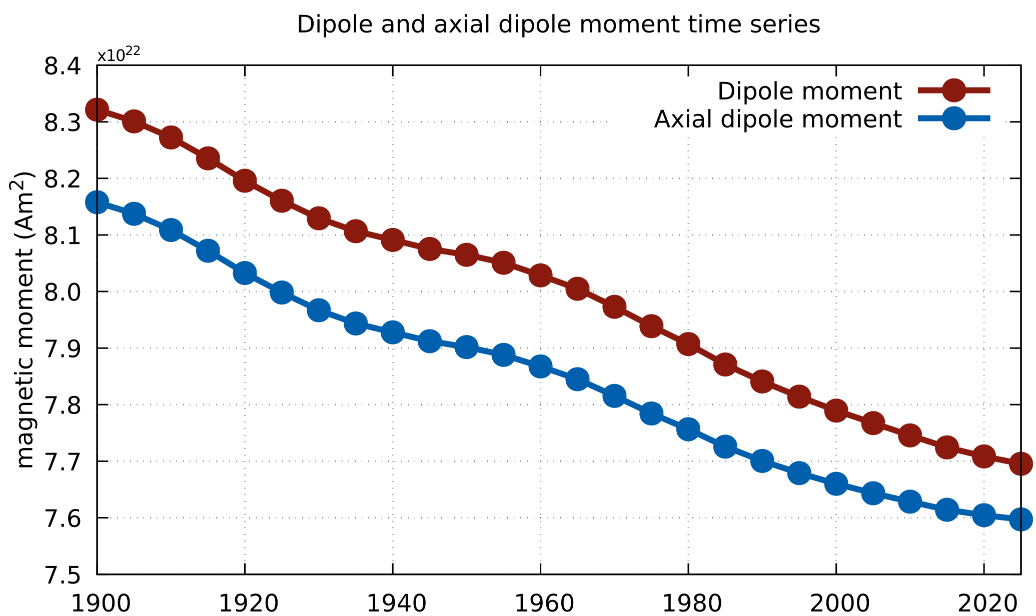

Fig. 5 Dipole and axial dipole moment time series derived from IGRF-13. The value for 2025 is a forecast

ce/models_compass/igrf_calc.html and http://wdc.kugi.kyoto-u.ac.jp/igrf/point/index.html

Archive of previous generations of IGRF: https://www.ngdc.noaa.gov/IAGA/vmod/igrf_old_models.html

Candidate models contributing to IGRF-13 and task force evaluation reports: https://www.ngdc.noaa.gov/IAGA/vmod/IGRF13/

Acknowledgements

The European Space Agency (ESA) is gratefully acknowledged for providing access to the Swarm magnetic field data and for making it possible for IPGP and CEA-Léti to derive the additional ASM-V experimental data from the CNES funded ASM instrument, all used in this work. The China National Space Administration and the China Earthquake Administration are acknowledged for providing access to CSES magnetometer data. The results presented in this paper rely on data collected at magnetic observatories. We thank the national institutes that support them and INTERMAGNET for promoting high standards of magnetic observatory practice (www.intermagnet.org).

Authors' contributions
P. Alken is chair of the IAGA DIV V-MOD (2019-2023) and initiated, coordinated and organized the call and delivery of the 13th generation of the IGRF. E. Thébault is former chair (2015–2019). C. Beggan is presently co-chair (2019–2023). PA, ET and CDB wrote the manuscript based on the analyses of the contributing co-authors. All other authors contributed modeling results and/or detailed technical analyses for IGRF-13. All authors have read and approved the final manuscript.

Funding
The Swarm and Cryosat-2 missions are supported by the European Space Agency (ESA). The Ørsted mission was made possible by extensive support from the Danish government, NASA, ESA, CNES, DARA, and the Thomas B. Thriges Foundation. The CHAMP mission was sponsored by the Space Agency of the German Aerospace Center (DLR) through funds of the Federal Ministry of Economics and Technology, following a decision of the German Federal Parliament (grant code 50EE0944). The SAC-C mission was made possible by a collaboration between the Comisión Nacional de Actividades Espaciales (CONAE), NASA/JPL, and the Danish Space Research Institute. The CSES mission is funded by the China National Space Administration (CNSA) and the China Earthquake Administration (CEA). The international network of geomagnetic observatories is supported by numerous institutes, staff, and INTERMAGNET. The French contribution to this work was supported by the French Centre National des Etudes Spatiales (CNES) in the framework of the program "Exploitation de la mission satellitaire européenne Swarm."

Availability of data and materials
Swarm and Cryosat-2 data are available from https://earth.esa.int/web/guest/swarm/data-access. CHAMP data can be obtained from http://isdc.gfz-potsdam.de. Ørsted and SAC-C data are available from https://www.space.dtu.dk/english/research/scientific_data_and_models/magnetic_satellites. CSES data is available from http://www.leos.ac.cn. INTERMAGNET data is available from https://www.intermagnet.org.

Competing interests
The authors declare that they have no competing interests.

Author details
[1] Cooperative Institute for Research in Environmental Sciences, University of Colorado Boulder, 325 Broadway, E/NE42, Boulder, CO 80305, USA. [2] NOAA National Centers for Environmental Information, Boulder, CO, USA. [3] Laboratoire de Planétologie et Géodynamique, UMR 6112, Université de Nantes, Université d'Angers, CNRS, Nantes, France. [4] British Geological Survey, The Lyell Centre, Research Avenue South, Edinburgh EH14 4AP, UK. [5] Division of Geomagnetism, DTU Space, Technical University of Denmark, Centrifugevej 356, Kongens Lyngby 2800, Denmark. [6] Université de Paris, Institut de Physique du Globe de Paris, CNRS, 75005 Paris, France. [7] Univ. Grenoble Alpes, Univ. Savoie Mont Blanc, CNRS, IRD, IFSTTAR, ISTerre, 38000 Grenoble, France. [8] School of Earth and Environment, University of Leeds, Leeds LS2 9JT, UK. [9] University of Newcastle, Newcastle upon Tyne NE1 7RU, UK. [10] GFZ German Research Centre for Geosciences, Telegrafenberg, 14473 Potsdam, Germany. [11] Division of Earth and Planetary Sciences, Graduate School of Science, Kyoto University, Kitashirakawa Oiwake-cho, Sakyo-ku, Kyoto 606-8502, Japan. [12] Institut de Physique du Globe de Strasbourg, Université de Strasbourg/EOST, CNRS, UMR 7516, Strasbourg, France. [13] Institute of Crustal Dynamics, China Earthquake Administration, Beijing, China. [14] State Key Laboratory of Space Weather, National Space Science Center, Chinese Academy of Sciences, Beijing 100190, China. [15] Space Research Institute, Austrian Academy of Sciences, Schmiedlstraße 6, Graz, Austria. [16] CEA-Leti, Minatec Campus, Grenoble, France. [17] Pushkov Institute of Terrestrial Magnetism, Ionosphere and Radio Wave Propagation, Kaluzhskoe Hwy 4, Moscow, Russia. [18] Earthquake and Volcano Research Center, Graduate School of Environmental Studies, Nagoya University, D2-2, Furo-cho, Chikusa-ku, Nagoya, Aichi 464-8601, Japan. [19] Department of Statistical Modeling, The Institute of Statistical Mathematics, 10-3 Midori-cho, Tachikawa, Tokyo 190-8562, Japan. [20] Department of Planetology, Graduate School of Science, Kobe University, 1-1, Rokkodai-cho, Nada-ku, Kobe, Hyogo 657-8501, Japan. [21] Max Planck Institute for Solar System Research, Justus-von-Liebig-Weg 3, 37077 Göttingen, Germany. [22] University of Potsdam, Am Neuen Palais 10, Potsdam, Germany. [23] NASA/Goddard Space Flight Center, Greenbelt, MD, USA. [24] Universidad Complutense de Madrid, Madrid, Spain. [25] Geoscience Institute IGEO, Madrid, Spain. [26] Observatori de l'Ebre (OE), Univ. Ramon Llull - CSIC, Roquetes, Spain. [27] Centre National d'Etudes Spatiales, Paris, France. [28] Institute of Geophysics, Department of Earth Sciences, ETH Zurich, Sonneggstrasse 5, Zurich 8092, Switzerland.

Appendix 1: World data system

WORLD DATA SERVICE FOR GEOPHYSICS, BOULDER
NOAA National Centers for Environmental Information
325 Broadway, E/NE42, Boulder, CO, 80305-3328, UNITED STATES OF AMERICA
TEL: +1 303 497 5480
FAX: +1 303 497 6513
EMAIL: geomag.models@noaa.gov
INTERNET: https://www.ngdc.noaa.gov

WORLD DATA CENTER FOR GEOMAGNETISM, COPENHAGEN
Technical University of Denmark, DTU Space, Centrifugevej, Building 356, DK 2800, Kgs. Lyngby, DENMARK
TEL: +45 4525 9713
FAX: +45 4525 9701
EMAIL: anna@space.dtu.dk
INTERNET: http://www.space.dtu.dk/English/Research/Scientific_data_and_models

WORLD DATA CENTRE FOR GEOMAGNETISM, EDINBURGH
British Geological Survey
The Lyell Centre
Edinburgh, EH14 4AP
UNITED KINGDOM
TEL: +44 131 667 1000
EMAIL: wdcgeomag@bgs.ac.uk
INTERNET: http://www.wdc.bgs.ac.uk

WORLD DATA CENTER FOR GEOMAGNETISM, KYOTO
Data Analysis Center for Geomagnetism and Space Magnetism
Graduate School of Science, Kyoto University
Kitashirakawa-Oiwake Cho, Sakyo-ku
Kyoto, 606-8502, JAPAN
TEL: +81 75 753 3929
FAX: +81 75 722 7884
EMAIL: toh@kugi.kyoto-u.ac.jp
INTERNET: http://wdc.kugi.kyoto-u.ac.jp

WORLD DATA CENTER FOR SOLID EARTH PHYSICS, MOSCOW
Geophysical Center of the Russian Academy of Sciences
Molodezhnaya, 3
Moscow, 119296, RUSSIA
TEL: +7 495 930 56 49
FAX: +7 495 930 05 06
EMAIL: wdcsep@wdcb.ru
INTERNET: http://www.wdcb.ru/sep/index.html

WORLD DATA CENTRE FOR GEOMAGNETISM, MUMBAI
Indian Institute of Geomagnetism
New Panvel(W), Navi Mumbai, 410 218, INDIA
TEL: +91 22 274807 66
FAX: +91 22 274807 62
EMAIL: wdc@iigs.iigm.res.in
INTERNET: http://wdciig.res.in

Received: 11 May 2020 Accepted: 3 October 2020
Published online: 11 February 2021

References

Alken P, Chulliat A, Nair M (2020a) NOAA/NCEI and University of Colorado candidate models for IGRF-13. Earth Planets Space. https://doi.org/10.1186/s40623-020-01313-z

Alken P, Thébault E, Beggan C, Aubert J, Baerenzung J, Brown W, Califf S, Chulliat A, Cox G, Finlay CC, Fournier A, Gillet N, Hammer MD, Holschneider M, Hulot G, Korte M, Lesur V, Livermore P, Lowes F, Macmillan S, Nair M, Olsen N, Ropp G, Rother M, Schnepf NR, Stolle C, Toh H, Vervelidou F, Vigneron P, Wardinski I (2020b) Evaluation of candidate models for the 13th International Geomagnetic Reference Field. Earth Planets Space. https://doi.org/10.1186/s40623-020-01281-4

Baerenzung J, Holschneider M, Wicht J, Lesur V, Sanchez S (2020) The Kalmag model as a candidate for IGRF-13. Earth Planets Space. https://doi.org/10.1186/s40623-020-01295-y

Barraclough DR (1987) International geomagnetic reference field: the fourth generation. Phys Earth Planet Interiors 48(3):279–292. https://doi.org/10.1016/0031-9201(87)90150-6

Barraclough DR, Mundt W, Barker FS, Barton CE, Golovkov VP, Hood PJ, Lowes FJ, Peddie NW, Gui-zhong Q, Srivastava SP, Winch DE, Yukutake T, Zidarov DP, Chen-chang A, Estes RH, Kerridge DJ, Langel RA, Quinn JM, Sabaka TJ, Verhoef J (1987) International Geomagnetic Reference Field Revision 1987. J Geomagnetism Geoelectricity 39(12):773–779. https://doi.org/10.5636/jgg.39.773

Barton CE (1997) International geomagnetic reference field: The seventh generation. J Geomagnetism Geoelectricity 49(2–3):123–148. https://doi.org/10.5636/jgg.49.123

Brown W, Beggan CD, Cox G, Macmillan S (2020) The BGS candidate models for IGRF-13 with a retrospective analysis of IGRF-12 secular variation forecasts. Earth Planets Space. https://doi.org/10.1186/s40623-020-01301-3

Cain JC, Cain SJ (1971) Derivation of the International Geomagnetic Reference Field IGRF(10/68). Tech. Rep. D-6237, NASA

Colomb F, Alonso C, Hofmann C, Nollmann I (2004) SAC-C mission, an example of international cooperation. Adv Space Res 34(10):2194–2199. https://doi.org/10.1016/j.asr.2003.10.039

Constable C, Korte M (2015) Centennial to millennial-scale geomagnetic field variations. In: Schubert G (ed) Treatise on Geophysics, vol 5, 2nd edn. Amsterdam, Elsevier. pp 309–341

Finlay CC, Maus S, Beggan CD, Bondar TN, Chambodut A, Chernova TA, Chulliat A, Golovkov VP, Hamilton B, Hamoudi M, Holme R, Hulot G, Kuang W, Langlais B, Lesur V, Lowes FJ, Lühr H, Macmillan S, Mandea M, McLean S, Manoj C, Menvielle M, Michaelis I, Olsen N, Rauberg J, Rother M, Sabaka TJ, Tangborn A, Tøffner-Clausen L, Thébault E, Thomson AWP, Wardinski I, Wei Z, Zvereva TI (2010a) International Geomagnetic Reference Field: the eleventh generation. Geophys J Int 183(3):1216–1230. https://doi.org/10.1111/j.1365-246X.2010.04804.x, https://academic.oup.com/gji/article-pdf/183/3/1216/1785065/183-3-1216.pdf

Finlay CC, Maus S, Beggan CD, Hamoudi M, Lowes FJ, Olsen N, Thébault E (2010b) Evaluation of candidate geomagnetic field models for IGRF-11. Earth Planets Space 62(10):8

Finlay CC, Kloss C, Olsen N, Hammer M, Tøffner-Clausen L, Grayver A, Kuvshinov A (2020) The CHAOS-7 geomagnetic field model and observed changes in the South Atlantic Anomaly. Earth Planets Space. https://doi.org/10.1186/s40623-020-01252-9

Fournier A, Aubert J, Lesur V, Ropp G (2020) A secular variation candidate model for IGRF-13 based on Swarm data and ensemble inverse geodynamo modelling. Earth Planets Space. https://doi.org/10.1186/s40623-020-01309-9

Friis-Christensen E, Lühr H, Hulot G (2006) Swarm: a constellation to study the Earth's magnetic field. Earth Planets Space 58(4):351–358

Huder L, Gillet N, Finlay CC, Hammer MD, Tchoungui H (2020) COV-OBS.x2: 180 yr of geomagnetic field evolution from ground-based and satellite observations. Earth Planets Space. https://doi.org/10.1186/s40623-020-01194-2

IAGA Division I Study Group (1975) International Geomagnetic Reference Field 1975. J Geomagnetism Geoelectricity 27(5):437–439. https://doi.org/10.5636/jgg.27.437

Langel RA (1992) International geomagnetic reference field: the sixth generation. J Geomagnetism Geoelectricity 44(9):679–707. https://doi.org/10.5636/jgg.44.679

Langel RA, Barraclough DR, Kerridge DJ, Golovkov VP, Sabaka TJ, Estes RH (1988) Definitive IGRF Models for 1945, 1950, 1955, and 1960. J Geomagnetism Geoelectricity 40(6):645–702. https://doi.org/10.5636/jgg.40.645

Laundal KM, Richmond AD (2017) Magnetic coordinate systems. Space Sci Rev 206(1–4):27–59

Lowes F (2000) An estimate of the errors of the IGRF/DGRF fields 1945–2000. Earth Planets Space 52(12):1207–1211

Macmillan S, Finlay CC (2011) The International Geomagnetic Reference Field. In: Mandea M, Korte M (eds) Geomagnetic Observations and Models, vol 5. Cham, Springer. pp 265–276

Macmillan S, Maus S (2005) International geomagnetic reference field–the tenth generation. Earth Planets Space 57(12):1135–1140. https://doi.org/10.1186/BF03351896

Macmillan S, Maus S, Bondar T, Chambodut A, Golovkov V, Holme R, Langlais B, Lesur V, Lowes F, Lühr H, Mai W, Mandea M, Olsen N, Rother M, Sabaka T, Thomson A, Wardinski I (2003) The 9th-Generation International Geomagnetic Reference Field. Geophys J Int 155(3):1051–1056. https://doi.org/10.1111/j.1365-246X.2003.02102.x, https://academic.oup.com/gji/article-pdf/155/3/1051/6103811/155-3-1051.pdf

Mandea M, Macmillan S (2000) International geomagnetic reference field–the eighth generation. Earth Planets Space 52(12):1119–1124. https://doi.org/10.1186/BF03352342

Maus S, Macmillan S, Chernova T, Choi S, Dater D, Golovkov V, Lesur V, Lowes F, Lühr H, Mai W, McLean S, Olsen N, Rother M, Sabaka T, Thomson A, Zvereva T (2005) The 10th-Generation International Geomagnetic Reference Field. Geophys J Int 161(3):561–565. https://doi.org/10.1111/j.1365-246X.2005.02641.x, https://academic.oup.com/gji/article-pdf/161/3/561/6065899/161-3-561.pdf

Merrill RT, McElhinny MW, McFadden PL (1996) The Magnetic Field of the Earth: Paleomagnetism, the core, and the deep mantle, International Geophysics Series, vol 63. Cambridge, Academic Press,

Metman MC, Beggan CD, Livermore PW, Mound JE (2020) Forecasting yearly geomagnetic variation through sequential estimation of core flow and magnetic diffusion. Earth Planets Space. https://doi.org/10.1186/s40623-020-01193-3

Minami T, Nakano S, Lesur V, Takahashi F, Matsushima M, Shimizu H, Nakashima R, Taniguchi H, Toh H (2020) A candidate secular variation model for

IGRF-13 based on MHD dynamo simulation and 4DEnVar data assimilation. Earth Planets Space. https://doi.org/10.1186/s40623-020-01253-8
Olsen N, Holme R, Hulot G, Sabaka T, Neubert T, Tøffner-Clausen L, Primdahl F, Jørgensen J, Léger JM, Barraclough D, Bloxham J, Cain J, Constable C, Golovkov V, Jackson A, Kotzé P, Langlais B, Macmillan S, Mandea M, Merayo J, Newitt L, Purucker M, Risbo T, Stampe M, Thomson A, Voorhies C (2000) Ørsted Initial Field Model. Geophys Res Lett 27(22):3607–3610. https://doi.org/10.1029/2000GL011930, https://agupubs.onlinelibrary.wiley.com/doi/abs/10.1029/2000GL011930, https://agupubs.onlinelibrary.wiley.com/doi/pdf/10.1029/2000GL011930
Panovska S, Korte M, Constable CG (2019) One hundred thousand years of geomagnetic field evolution. Rev Geophys 57(4):1289–1337. https://doi.org/10.1029/2019RG000656
Pavón-Carrasco FJ, Marsal S, Torta JM, Catalán M, Martín-Hernández F, Tordesillas JM (2020) Bootstrapping Swarm and observatory data to generate candidates for the DGRF and IGRF-13. Earth Planets Space. https://doi.org/10.1186/s40623-020-01198-y
Peddie NW (1982) International Geomagnetic Reference Field: the Third Generation. J Geomagnetism Geoelectricity 34(6):309–326. https://doi.org/10.5636/jgg.34.309
Petrov VG, Bondar TN (2020) IZMIRAN sub-model for IGRF-13. Earth Planets Space. https://doi.org/10.1186/s40623-020-01312-0
Reigber C, Lühr H, Schwintzer P (2002) CHAMP mission status. Adv Space Res 30(2):129–134
Ropp G, Lesur V, Baerenzung J, Holschneider M (2020) Sequential modelling of the Earth's core magnetic field. Earth Planets Space. https://doi.org/10.1186/s40623-020-01230-1
Rother M, Korte M, Morschhauser A, Vervelidou F, Matzka J, Stolle C (2020) The Magnum core field model as a parent for IGRF-13, and the recent evolution of the South Atlantic Anomaly. Earth Planets Space. https://doi.org/10.1186/s40623-020-01277-0
Sabaka TJ, Tøffner-Clausen L, Olsen N, Finlay CC (2020) CM6: A Comprehensive Geomagnetic Field Model Derived From Both CHAMP and Swarm Satellite Observations. Earth Planets Space. https://doi.org/10.1186/s40623-020-01210-5
Sanchez S, Wicht J, Bärenzung J (2020) Predictions of the geomagnetic secular variation based on the ensemble sequential assimilation of geomagnetic field models by dynamo simulations. Earth Planets Space. https://doi.org/10.1186/s40623-020-01279-y
Shen X, Zhang X, Yuan S, Wang L, Cao J, Huang J, Zhu X, Piergiorgio P, Dai J (2018) The state-of-the-art of the China Seismo-Electromagnetic Satellite mission. Science China Technological Sciences 61(5):634–642
Tangborn A, Kuang W, Sabaka TJ, Yi C (2020) Geomagnetic secular variation forecast using the NASA GEMS ensemble Kalman filter: A candidate model for IGRF 2020. Earth, Planets and Space. https://doi.org/10.1186/s40623-020-01324-w
Terra-Nova F, Amit H, Choblet G (2019) Preferred locations of weak surface field in numerical dynamos with heterogeneous core-mantle boundary heat flux: consequences for the South Atlantic Anomaly. Geophysical Journal International 217(2):1179–1199
Thébault E, Finlay CC, Beggan CD, Alken P, Aubert J, Barrois O, Bertrand F, Bondar T, Boness A, Brocco L, Canet E, Chambodut A, Chulliat A, Coïsson P, Civet F, Du A, Fournier A, Fratter I, Gillet N, Hamilton B, Hamoudi M, Hulot G, Jager T, Korte M, Kuang W, Lalanne X, Langlais B, Léger JM, Lesur V, Lowes FJ, Macmillan S, Mandea M, Manoj C, Maus S, Olsen N, Petrov V, Ridley V, Rother M, Sabaka TJ, Saturnino D, Schachtschneider R, Sirol O, Tangborn A, Thomson A, Tøffner-Clausen L, Vigneron P, Wardinski I, Zvereva T (2015) International Geomagnetic Reference Field: the 12th generation. Earth, Planets, and Space 67:79. https://doi.org/10.1186/s40623-015-0228-9
Vigneron P, Hulot G, Leger JM, Jager T (2019) Core field modelling using ASM-V vector data on board the Swarm satellites. In: 9th Swarm data quality workshop, Faculty of Civil Engineering, CTU, Prague, Czech Republic, 16–20 September 2019
Wardinski I, Saturnino D, Amit H, Chambodut A, Langlais B, Mandea M, Thébault E (2020) Geomagnetic core field models and secular variation forecasts for the 13th International Geomagnetic Reference Field (IGRF-13). Earth Planets Space. https://doi.org/10.1186/s40623-020-01254-7
Winch DE, Ivers DJ, Turner JPR, Stening RJ (2005) Geomagnetism and Schmidt quasi-normalization. Geophysical Journal International 160(2):487–504. https://doi.org/10.1111/j.1365-246X.2004.02472.x, https://academic.oup.com/gji/article-pdf/160/2/487/5970028/160-2-487.pdf
Yang Y, Hulot G, Vigneron P, Shen X, Zeren Z, Zhou B, Magnes W, Olsen N, Tøffner-Clausen L, Huang J, Zhang X, Wang L, Cheng B, Pollinger A, Lammegger R, Lin J, Guo F, Yu J, Wang J, Wu Y, Zhao X (2020) The CSES Global Geomagnetic Field Model (CGGM): An IGRF type global geomagnetic field model based on data from the China Seismo-Electromagnetic Satellite. Earth, Planets and Space. https://doi.org/10.1186/s40623-020-01316-w
Zmuda AJ (1971a) The International Geomagnetic Reference Field: Introduction. Bull Int Assoc Geomag Aeronomy 28:148–152
Zmuda AJ (1971b) World magnetic survey 1957-1969. IAGA Bulletin No 28

Publisher's Note

Springer Nature remains neutral with regard to jurisdictional claims in published maps and institutional affiliations.